Gondwana Research 23 (2013) 1631–1645

Contents lists available at SciVerse ScienceDirect

Gondwana Research

journal homepage: www.elsevier.com/locate/gr

Triassic river systems and the paleo-Pacific margin of northwestern Pangea

Elizabeth L. Miller [a,*], Alexey V. Soloviev [b], Andrei V. Prokopiev [c], Jaime Toro [d], Dan Harris [d], Alexander B. Kuzmichev [b], George E. Gehrels [e]

[a] Department of Geological and Environmental Sciences, Stanford University, Stanford, CA 94305, USA
[b] Geological Institute, Russian Academy of Sciences, Moscow, Russia
[c] Diamond and Precious Metal Geology Institute, Siberian Branch, Russian Academy of Sciences, Yakutsk, Russia
[d] Dept. Geology and Geography, West Virginia University, Morgantown, WV, USA
[e] Department of Geosciences, University of Arizona, Tucson, Arizona 85721, USA

ARTICLE INFO

Article history:
Received 18 March 2012
Received in revised form 16 August 2012
Accepted 22 August 2012
Available online 18 September 2012

Handling editor: I. Safonova

Keywords:
Arctic
Alaska
Russia
Detrital zircon geochronology
Paleogeography

ABSTRACT

Detrital zircon U–Pb ages from Triassic strata exposed in the circum-Arctic, analyzed by LA-ICP-MS and SHRIMP-RG, are compared at the regional scale to better understand the paleogeography of northern Pangea and help restore rift opening of the Arctic. Data sets are compared based on their zircon age distributions, cumulative age probability plots, and the K–S test. Three major source regions are characterized. These fed clastic material to transcontinental river systems that transported material from the highlands of northwestern Pangea to its once continuous paleo-Pacific continental margin. The paleo-Lena River System was fed from sources in the Baikalian and Altay-Sayan mountainous regions of Siberia. Zircon populations are characterized by a limited number of Precambrian zircons (~1.8–2.0 Ga with fewer ~2.5–3.0 Ga), lack of 0.9–1.8 Ga zircons, and a dominant 480–500 Ma and 290–300 Ma age population. The paleo-Taimyr River System was sourced from the Uralian orogenic belt region and deposited along a rifted portion of the Siberia–Baltica margin beginning in the Permo–Triassic. Precambrian zircon populations are similar to those of the paleo-Lena system, and samples closest to Siberia have similar populations in the 480–500 Ma and 290–300 Ma age ranges. Chukotka, Wrangel Island and Lisburne Hills, Alaska, have sparse ages between 900 and 1800 Ma, Ordovician ages are younger (~440–450 Ma), and, along with abundant ~300 Ma ages, they contain ~250–260 Ma and lesser ~215–235 Ma zircons, interpreted as derived from silicic volcanic centers associated with Permo–Triassic to Triassic continental flood basalt provinces in Siberia, Taimyr and Kara Sea region. The trans-Laurentian River System was likely fed by rift-related uplift along the proto North Atlantic/Arctic margin and delivered sediment to the Cordilleran margin of Pangea. These samples have no significant upper Paleozoic zircons and have a much broader age range of Precambrian zircons.

1. Introduction

Northern Pangea was fully assembled in the Early Permian after Siberia joined Baltica and Laurentia along the Uralian suture (Fig. 1) (e.g. Ziegler, 1988; Nikishin et al., 1996; Lawver et al., 2002). Its stability, however, was short-lived. The eruption of the Siberian traps and rifting along the western flank of the earlier Uralian suture created a broad aborted rift zone (the West Siberian Basin) that extended oceanward into inferred paleo-Pacific back-arc basins (Fig. 1; e.g. Nikishin et al., 2002; Reichow et al., 2009). In the North Atlantic/Artic region, the site of the older Caledonian orogenic belt also experienced rift-related uplift and formation of fault-bound basins beginning as early as the Permian and continuing into the Triassic. Rifting eventually led to continental break-up and formation of the North Atlantic later in the Cretaceous (Fig. 1; e.g. Ziegler, 1988; Nikishin et al., 2002).

This overall paleogeography (Fig. 1) dictated source regions for Triassic depositional systems and controlled the location and configuration of major river systems that carried clastic material to Pangea's northern paleo-Pacific continental margin (Fig. 1). Today, these siliciclastic deposits crop out in younger fold belts or remain deeply buried in basins (Fig. 2). Rifting and plate motions associated with the formation of the Cretaceous and Tertiary Arctic Ocean basins have severed many of these deposits from their original sources, making it more difficult to decipher their ancient Triassic paleogeography (Fig. 2).

U–Pb detrital zircon geochronology is a rapidly evolving and powerful tool for determining the provenance and maximum depositional age of clastic strata. The increased availability and speed of data collection by the laser ablation-ICP-mass spectrometers have generated increasingly larger data sets of this sort (e.g. Davis et al., 2003; Kostler and Sylvester, 2003; Gehrels, 2012). This method is effective

* Corresponding author. Tel.: +1 650 7231149.
E-mail address: elmiller@stanford.edu (E.L. Miller).

1342-937X/$ – see front matter © 2012 International Association for Gondwana Research. Published by Elsevier B.V. All rights reserved.
http://dx.doi.org/10.1016/j.gr.2012.08.015

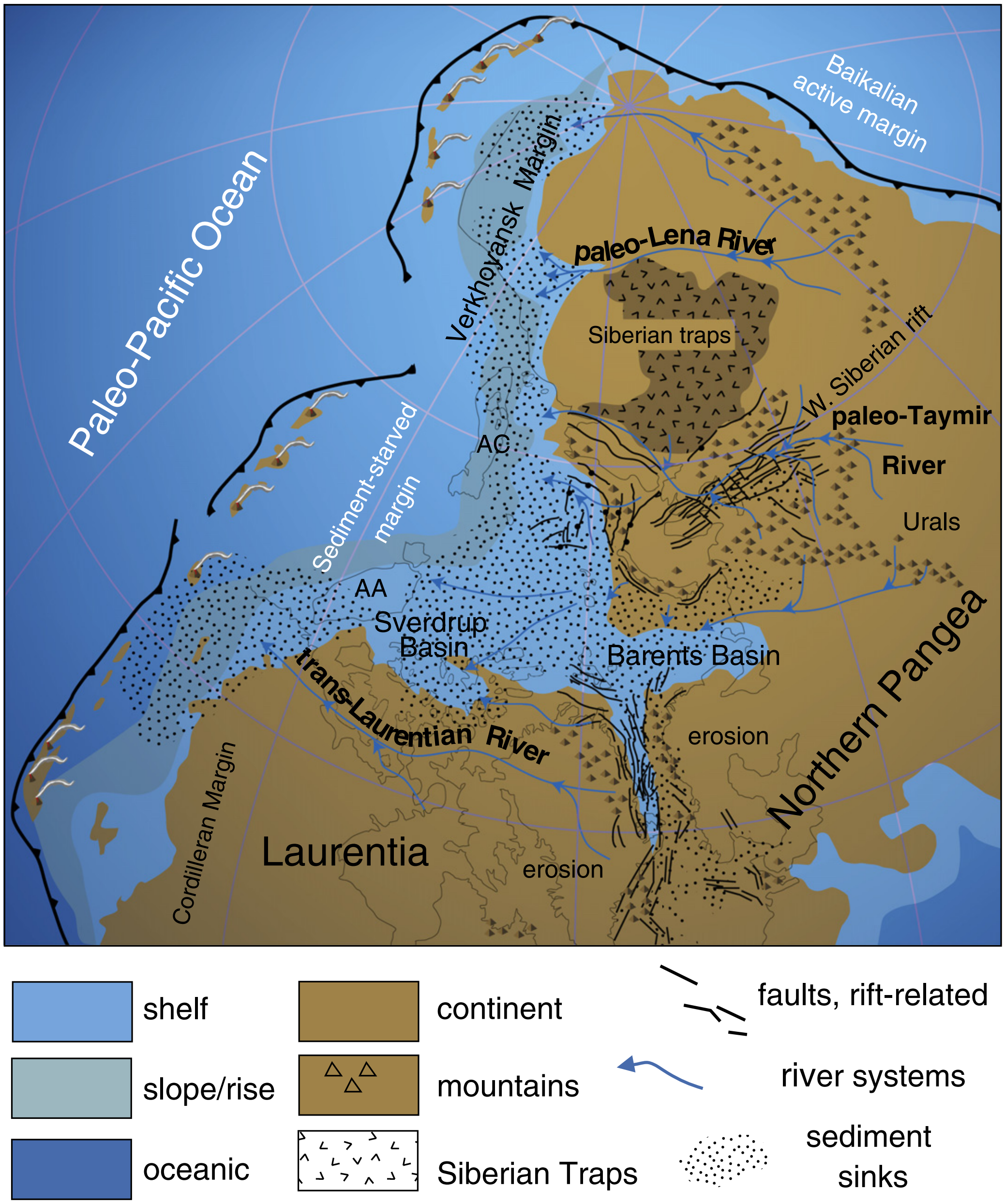

Fig. 1. Simplified paleogeography of northern Pangea in the Permo–Triassic to Early Triassic based on Lawver et al.'s (2002) Middle (240 Ma) to Late (210 Ma) reconstruction. Areas of shelf and continents, rift-related faults and mountains after Nikishin et al. (1996) and Ziegler (1988). Arctic Alaska (AA) restored following Lawver et al. (2002). The general region of Chukotka (AC) is restored after Miller et al. (2006, 2010, this paper). Proposed river systems of northern Pangea and offshore depositional "sinks" are portrayed in highly schematic form. Offshore island arcs and subduction zones are inferred. For discussion see text.

at testing and establishing the first-order coherency and source regions of large clastic depositional systems, enabling us to reconstruct ancient paleogeographies and tectonic events now obscured by younger deformational events and plate motions (e.g. Rino et al., 2008; Condie et al., 2009; Dickinson and Gehrels, 2010; Nebel-Jacobsen et al., 2011; Babinski et al., 2012).

This study of Triassic strata and their detrital zircon populations was initiated to determine how effective this approach might be in elucidating the rift opening geometry and history of the Arctic Ocean basins (e.g. Miller et al., 2006). Additional published data (Miller et al., 2010) and new results (this paper), when added to a growing number of regional studies (e.g. Beranek et al., 2010; Omma et al., 2011), provide a clearer and broader view of what was once the paleogeography of northern Pangea in the Triassic. Increased interest in the geology and natural resources of the Arctic has led to a series of new models for the plate tectonic evolution of the Arctic Ocean's Amerasia Basin (Fig. 2) (e.g. Kuzmichev, 2009; Miller et al., 2010; Colpron and Nelson, 2011; Golonka, 2011; Grantz et al., 2011; Lawver et al., 2011). The combined data set discussed here and the conclusions drawn from this data, although evolving, provide a solid basis for building and testing paleogeographic models and plate tectonic reconstructions of the Arctic.

2. Analytical methods and data analysis

The locations of the samples analyzed and discussed are shown in Fig. 2 and their exact locations and ages are listed in Appendix 1A. Most samples were collected from paleontologically dated Triassic stratigraphic successions (e.g. Sosunov et al., 1982; Harrison et al., 2008; Appendix 1A). Triassic strata in the New Siberian Islands

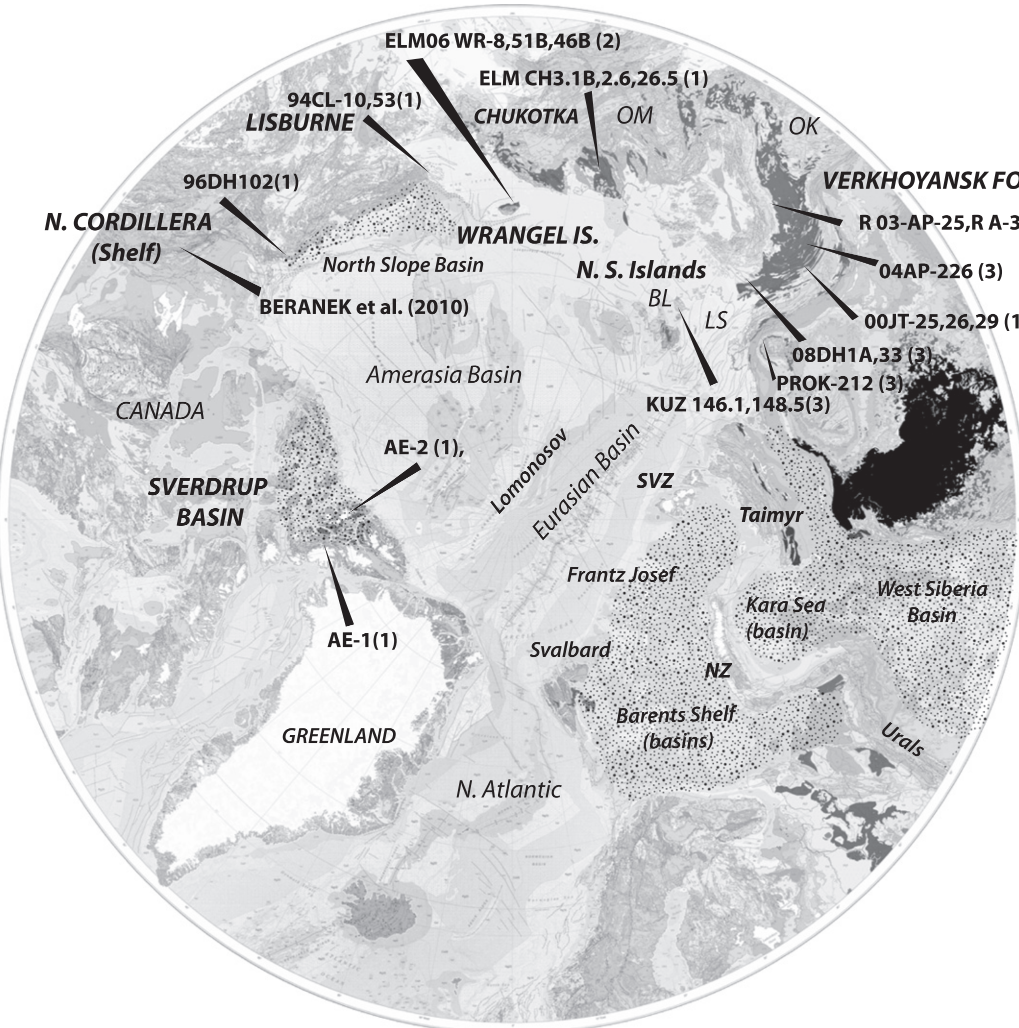

Fig. 2. Present-day outcrop distribution of Triassic sediments (gray) and Permo–Triassic to Triassic flood basalts (black) in the circum-Arctic and location of samples discussed in text. Base map after Harrison et al. (2008). Accumulations of Triassic strata in the subsurface after Grantz et al. (2011) (dot pattern). Many Triassic outcrops too thin to display. Sample data: 1 — published in Miller et al. (2006); 2 — published in Miller et al. (2010); 3 — this paper. Abbreviations: BL, Bolshoi Lyakov Island; LS, Laptev Sea; N.S., New Siberia Islands; NZ, Novaya Zemlya; OK, Okhotsk terrane; OM, Omolon terrane; SVZ, Severnaya Zemlya.

(Novosibirskije ostrova) and Chukotka (the Arctic coast of NE Russia west of the Bering Strait) are the most deformed and metamorphosed and their paleontological age and position in the stratigraphic section are not as well known (Fig. 2; Appendix 1, part A). Published analyses versus new analyses are designated in Fig. 2. Analytical methods, U–Pb data tables and concordia diagrams for new analyses are included in Appendix 1 (parts B, C and D for ICPMS analyses) and Appendix 2 (parts A, B and C for SHRIMP-RG analyses). Most of the U–Pb detrital zircon ages compared here were collected at the University of Arizona LA-ICP-MS LaserChron facility except for sample KUZ146.1 (New Siberian Islands, analyzed by SHRIMP-RG) (Appendix 2). Sample preparation, data collection, processing and analysis methods follow those reported in Miller et al. (2006, 2010). Approximately 100 detrital zircons are randomly dated from a dump mount of an aliquot of the zircon separate as detailed in Fig. 3. The U–Pb ages of zircons from four samples were further investigated using the Stanford-USGS SHRIMP-RG (Appendix 2). These additional analyses were carried out on hand-picked euhedral portions of the detrital zircon populations with the goal of more directly determining the range of ages represented by first-cycle detrital zircons as illustrated in Fig. 3. Dating of the most euhedral portions of the zircon populations can help to better determine the youngest age range of zircons in the sample and can also be used to establish the age range of the suite of igneous rocks in the source area that are (together) undergoing erosion and transport for the first time. Other data included in our analysis and discussions are data reported by Beranek et al. (2010) from the northernmost Canadian Cordillera (Fig. 2). We discuss but do not include in our analysis Omma et al.'s (2011) data from the Sverdrup Basin. Other regions where detrital zircon U–Pb ages have been reported from Triassic strata in abstract form include Franz Josef Land (Pease et al., 2007, 2012), Taimyr (Larionov, pers. com., 2007) and Svalbard (Bue et al., 2012).

All of the published and new data were compiled and compared using age histograms and relative age probability plots which are included in Appendix 3. Main age groups, age peaks and youngest age groups were determined with the “Age Pick” algorithm available at www.geo.arizona.edu/alc and are also included in Appendix 3. The data are presented in cumulative age probability plots in Fig. 4 and further compared in terms of their K–S test P values in Fig. 5. The K–S test (Kolmogorov–Smirnov test) uses the error from the calculated cumulative distribution functions (Fig. 4) (Press et al., 1992; Guynn and Gehrels, 2010). Output values “P” from the K–S test use the vertical separation D between two cumulative probability plots (Fig. 4). The K–S statistic measures the probability that two age distribution curves are not drawn from the same original population. The P value is the probability that two samples are not statistically different. A P value >0.05 yields 95% confidence that the two samples are not

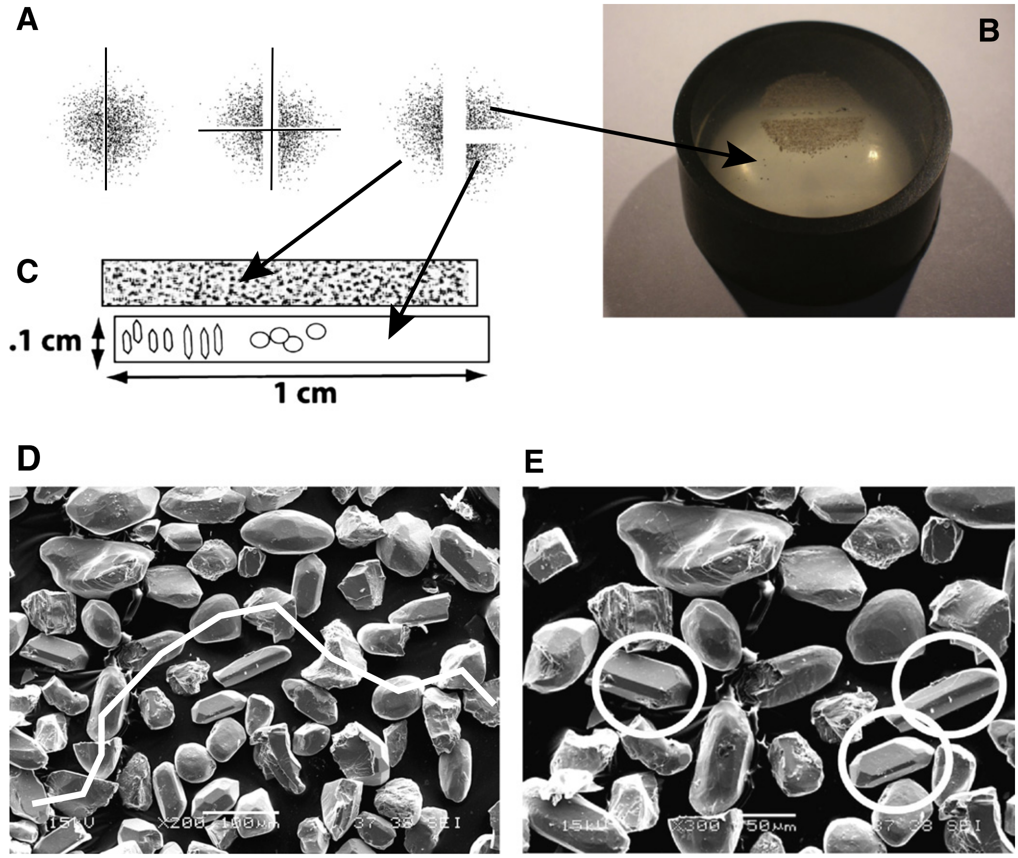

Fig. 3. Methodology for analyses of detrital zircons. A. Splitting the zircon grains. B. Typical detrital zircon sample mount at the University of Arizona LaserChron Center, where an aliquot of the sample is "dump" mounted (with a row of standards in the center). C. Detrital zircon dump mount for analysis with the SHRIMP-RG (top slot) and hand-picked euhedral (as well as most rounded) part of the zircon population (bottom slot). D. Random walk approach to dating dump-mounted detrital zircons. E. SEM image of zircon population with the most euhedral grains circled. Selection criteria for euhedral zircons included sharp crystal edges, flat reflective crystal facets and large length to width ratios, a proxy for first cycle zircons.

statistically different. Because P is calculated using "D", the calculation is sensitive to the proportion of ages present (e.g. all of the same ages might be represented, but in differing proportions, leading to a large "D"). Thus the K–S test P values should be used in conjunction with the comparison of the shapes of cumulative age probability plots (Fig. 4).

The samples analyzed are from widespread geographic locations, geologic settings and from separate depositional basins. They are only broadly coeval, thus their geological context and setting is critical to this preliminary comparison. Despite this, our analysis indicates that meaningful differences exist between major source regions and the depositional systems that provided their detritus to the northern margin of Pangea in the Triassic. These differences can be used to test and develop more detailed, holistic plate reconstructions for the Triassic.

3. Results and discussion of data

The sets of cumulative age probability plots for all detrital zircon suites (Fig. 4A) are separated in groups based on their geographic location, similarities in their detrital zircon populations (Fig. 4B, C, D, E and Appendix 3) and K–S test P values (Fig. 5). The data displayed in Fig. 4 highlight the key differences between three main groups of samples, collected respectively from 1) the Verkhoyansk margin of NE Russia, 2) Arctic Russia and Alaska including Big Lyakhov Island of the New Siberian Islands, Chukotka, Wrangel Island and the Lisburne Hills and 3) the northernmost Canadian Cordillera (Beranek et al., 2010). These three groups of samples all contrast with two individual (and fairly unique) samples collected from eastern Alaska and the Sverdrup Basin (Figs. 4 and 5). Below, we discuss the main groups of samples and their detrital zircon populations, how they compare and differ, and evaluate whether they once formed part of larger depositional systems that were subsequently disrupted by younger deformation and the rift opening of the Arctic Ocean basins (Fig. 2).

3.1. Verkhoyansk margin and the paleo-Lena River

The Verkhoyansk fold and thrust belt of NE Russia (Figs. 1, 2 and 6) contains one of the largest clastic sedimentary successions in the world, deposited along the eastern, paleo-North Pacific facing margin of the Siberian craton. This clastic succession was deposited following a major re-configuration of the margin by Late Devonian rifting, leaving an aulacogen, the Vilyui graben system, which became the paleo-Lena River valley (Fig. 6) (Gaiduk, 1988; Parfenov et al., 1995). Subsidence from Early Carboniferous (Mississippian) to Jurassic time led to the accumulation of a sedimentary prism up to 15 km thick along the Verkhoyansk margin (Fig. 6). A prior study of detrital zircons suggests this clastic wedge was sourced from the Baikalian and Altay-Sayan mountainous regions of southern Siberia, carried by the paleo-Lena River, delivering sediments to the paleo-Pacific margin of Siberia (Prokopiev et al., 2008) (Fig. 6). U–Pb ages of detrital zircons from three Triassic sandstone samples (Miller et al., 2006; Prokopiev et al., 2008) together with samples collected from southern exposures of continental shelf sandstones (sample 04-AP-226) and from the inferred deep-water equivalents of this shelf sequence (the Kular-Nera Slate belt, samples R03-AP-25 and RA-3/5-01) are

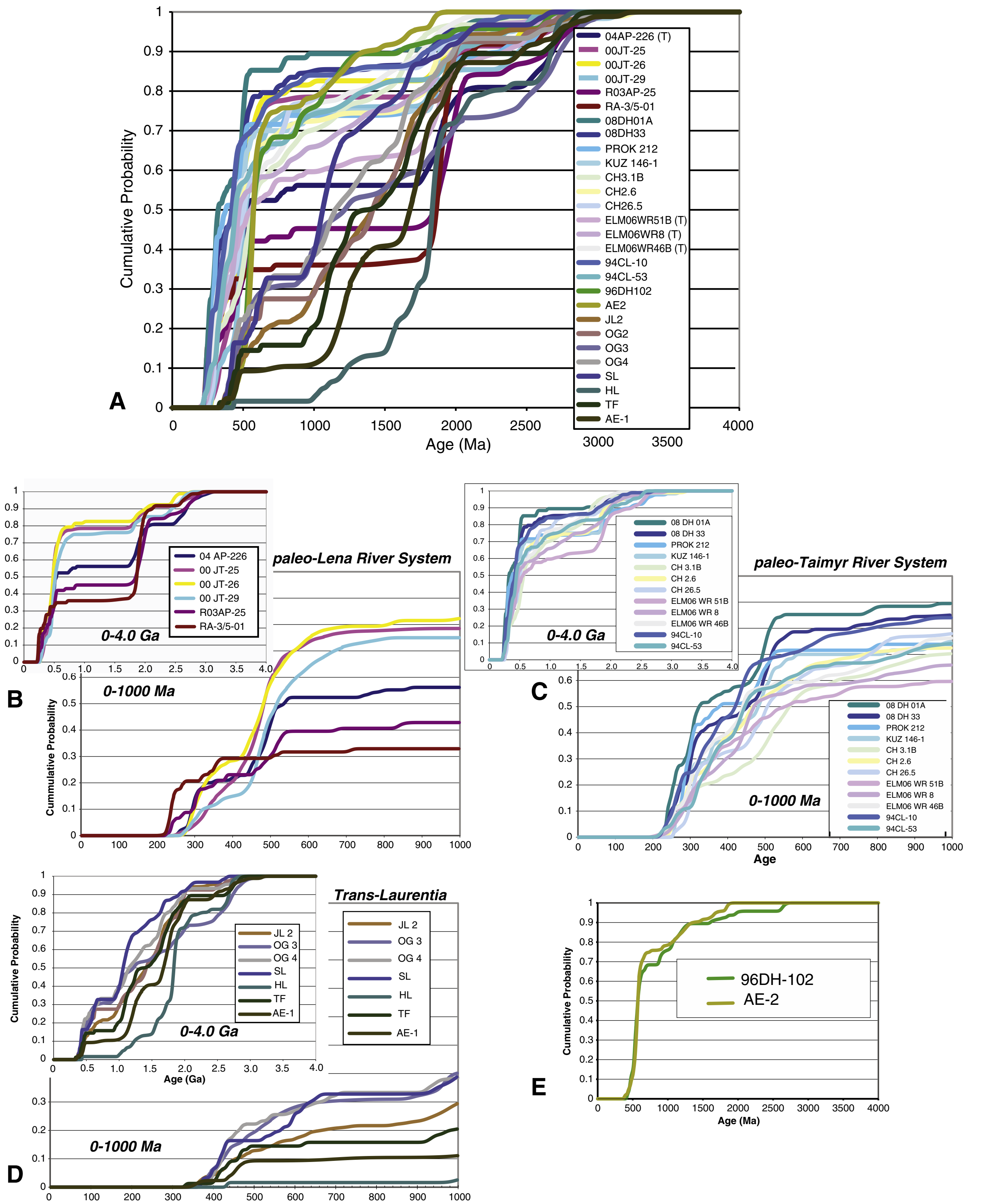

Fig. 4. Cumulative age probability plots for samples discussed. A. All Triassic samples together, B. Triassic from the Verkhoyansk region, C. Triassic from northernmost Siberia, Big Lyakhov Island (New Siberian Islands), Chukotka, Wrangel and Lisburne Hills, Alaska, D. Triassic from northernmost Canadian Cordillera (Beranek et al., 2010), E. Triassic from northeastern Alaska and the northern Sverdrup Basin. Note that plots for both the 0–1.0 Ga and 0–3.5 Ga intervals are shown for B, C and D. For discussion, see text.

shown in Figs 2 and 6. Continental and deltaic, shelf-facies sandstones inferred to have been fed by the paleo-Lena River system (Prokopiev et al., 2008) are characterized by Precambrian zircons that lie in the 1.8–2.0 Ga and 2.3–3.0 Ga age ranges with no zircons between ~1.8 and ~1.0 Ga (Fig. 4). The predominant ages of zircons in these samples are Paleozoic, and most are either Cambro–Ordovician–Silurian

	04AP-226	00JT-25	00JT-26	00JT-29	R03AP-25	RA-3/5-01	08DH01A	08DH33	PROK 212	KUZ 146-1	CH3.1B	CH2.6	CH26.5	ELM06WR51B	ELM06WR8	ELM06WR46B	94CL-10	94CL-53	96DH102	AE2	JL2	OG2	OG3	OG4	SL	HL	TF	AE-1
04AP-226		0.00	0.00	0.03	0.15	0.01	0.00	0.00	0.00	0.07	0.00	0.02	0.00	0.17	0.01	0.00	0.00	0.00	0.00	0.00	0.00	0.01	0.00	0.00	0.00	0.00	0.00	0.00
00JT-25	0.00		0.62	0.31	0.00	0.00	0.00	0.00	0.00	0.06	0.01	0.08	0.09	0.01	0.07	0.02	0.00	0.09	0.00	0.00	0.00	0.00	0.00	0.00	0.00	0.00	0.00	0.00
00JT-26	0.00	0.62		0.13	0.00	0.00	0.00	0.03	0.00	0.56	0.02	0.57	0.34	0.00	0.03	0.10	0.01	0.36	0.00	0.00	0.00	0.00	0.00	0.00	0.00	0.00	0.00	0.00
00JT-29	0.03	0.31	0.13		0.00	0.00	0.00	0.00	0.00	0.01	0.15	0.01	0.09	0.02	0.01	0.00	0.00	0.00	0.00	0.00	0.00	0.00	0.00	0.00	0.00	0.00	0.00	0.00
R03AP-25	0.15	0.00	0.00	0.00		0.33	0.00	0.00	0.00	0.00	0.00	0.00	0.00	0.01	0.00	0.00	0.00	0.00	0.00	0.00	0.00	0.02	0.08	0.00	0.00	0.00	0.00	0.00
RA-3/5-01	0.01	0.00	0.00	0.00	0.33		0.00	0.00	0.00	0.00	0.00	0.00	0.00	0.00	0.00	0.00	0.00	0.00	0.00	0.00	0.00	0.00	0.00	0.00	0.00	0.00	0.00	0.00
08DH01A	0.00	0.00	0.00	0.00	0.00	0.00		0.44	0.08	0.04	0.00	0.00	0.00	0.00	0.00	0.00	0.04	0.00	0.00	0.00	0.00	0.00	0.00	0.00	0.00	0.00	0.00	0.00
08DH33	0.00	0.00	0.03	0.00	0.00	0.00	0.44		0.37	0.46	0.00	0.08	0.04	0.00	0.01	0.04	0.33	0.03	0.00	0.00	0.00	0.00	0.00	0.00	0.00	0.00	0.00	0.00
PROK 212	0.00	0.00	0.00	0.00	0.00	0.00	0.08	0.37		0.32	0.00	0.07	0.04	0.01	0.01	0.17	0.20	0.00	0.00	0.00	0.00	0.00	0.00	0.00	0.00	0.00	0.00	0.00
KUZ 146-1	0.07	0.06	0.56	0.01	0.00	0.00	0.04	0.46	0.32		0.05	0.94	0.56	0.17	0.54	0.23	0.13	0.71	0.00	0.00	0.00	0.00	0.00	0.00	0.00	0.00	0.00	0.00
CH3.1B	0.00	0.01	0.02	0.15	0.00	0.00	0.00	0.00	0.00	0.05		0.04	0.40	0.00	0.03	0.00	0.00	0.01	0.01	0.01	0.00	0.00	0.00	0.00	0.00	0.00	0.00	0.00
CH2.6	0.02	0.08	0.57	0.01	0.00	0.00	0.00	0.08	0.07	0.94	0.04		0.56	0.27	0.66	0.58	0.17	0.76	0.00	0.00	0.00	0.00	0.00	0.00	0.00	0.00	0.00	0.00
CH26.5	0.00	0.09	0.34	0.09	0.00	0.00	0.00	0.04	0.04	0.56	0.40	0.56		0.01	0.23	0.06	0.00	0.17	0.00	0.00	0.00	0.00	0.00	0.00	0.00	0.00	0.00	0.00
ELM06WR51B	0.17	0.01	0.00	0.02	0.01	0.00	0.00	0.00	0.01	0.17	0.00	0.27	0.01		0.24	0.00	0.01	0.06	0.00	0.00	0.00	0.00	0.00	0.00	0.00	0.00	0.00	0.00
ELM06WR8	0.01	0.07	0.03	0.01	0.00	0.00	0.00	0.01	0.01	0.54	0.03	0.66	0.23	0.24		0.48	0.04	0.80	0.00	0.00	0.00	0.00	0.00	0.00	0.00	0.00	0.00	0.00
ELM06WR46B	0.00	0.02	0.10	0.00	0.00	0.00	0.00	0.04	0.17	0.23	0.00	0.58	0.06	0.00	0.48		0.18	0.53	0.00	0.00	0.00	0.00	0.00	0.00	0.00	0.00	0.00	0.00
94CL-10	0.00	0.00	0.01	0.00	0.00	0.00	0.04	0.33	0.20	0.13	0.00	0.17	0.00	0.01	0.04	0.18		0.36	0.00	0.00	0.00	0.00	0.00	0.00	0.00	0.00	0.00	0.00
94CL-53	0.00	0.09	0.36	0.00	0.00	0.00	0.00	0.03	0.00	0.71	0.01	0.76	0.17	0.06	0.80	0.53	0.36		0.00	0.00	0.00	0.00	0.00	0.00	0.00	0.00	0.00	0.00
96DH102	0.00	0.00	0.00	0.00	0.00	0.00	0.00	0.00	0.00	0.00	0.01	0.00	0.00	0.00	0.00	0.00	0.00	0.00		0.92	0.00	0.00	0.00	0.00	0.00	0.00	0.00	0.00
AE2	0.00	0.00	0.00	0.00	0.00	0.00	0.00	0.00	0.00	0.00	0.01	0.00	0.00	0.00	0.00	0.00	0.00	0.00	0.92		0.00	0.00	0.00	0.00	0.00	0.00	0.00	0.00
JL2	0.00	0.00	0.00	0.00	0.00	0.00	0.00	0.00	0.00	0.00	0.00	0.00	0.00	0.00	0.00	0.00	0.00	0.00	0.00	0.00		0.98	0.03	0.27	0.00	0.00	0.77	0.01
OG2	0.01	0.00	0.00	0.00	0.02	0.00	0.00	0.00	0.00	0.00	0.00	0.00	0.00	0.00	0.00	0.00	0.00	0.00	0.00	0.00	0.98		0.25	0.52	0.04	0.00	0.86	0.15
OG3	0.00	0.00	0.00	0.00	0.08	0.00	0.00	0.00	0.00	0.00	0.00	0.00	0.00	0.00	0.00	0.00	0.00	0.00	0.00	0.00	0.03	0.25		0.07	0.02	0.00	0.11	0.00
OG4	0.00	0.00	0.00	0.00	0.00	0.00	0.00	0.00	0.00	0.00	0.00	0.00	0.00	0.00	0.00	0.00	0.00	0.00	0.00	0.00	0.27	0.52	0.07		0.39	0.00	0.10	0.00
SL	0.00	0.00	0.00	0.00	0.00	0.00	0.00	0.00	0.00	0.00	0.00	0.00	0.00	0.00	0.00	0.00	0.00	0.00	0.00	0.00	0.00	0.04	0.02	0.39		0.00	0.02	0.00
HL	0.00	0.00	0.00	0.00	0.00	0.00	0.00	0.00	0.00	0.00	0.00	0.00	0.00	0.00	0.00	0.00	0.00	0.00	0.00	0.00	0.00	0.00	0.00	0.00	0.00		0.00	0.00
TF	0.00	0.00	0.00	0.00	0.00	0.00	0.00	0.00	0.00	0.00	0.00	0.00	0.00	0.00	0.00	0.00	0.00	0.00	0.00	0.00	0.77	0.86	0.11	0.10	0.02	0.00		0.09
AE-1	0.00	0.00	0.00	0.00	0.00	0.00	0.00	0.00	0.00	0.00	0.00	0.00	0.00	0.00	0.00	0.00	0.00	0.00	0.00	0.00	0.01	0.15	0.00	0.00	0.00	0.00	0.09	

PALEO LENA RIVER **PALEO TAIMYR RIVERS** **PALEO LAURENTIA RIVERS**

Fig. 5. P value results from the Kolmogorov–Smirnov statistical test for all samples discussed. White, P values less than 0.05 but greater than 0; yellow, P values greater than 0.05, darker yellow, P values >0.6. For discussion, see text.

or Carboniferous–Permian (Fig. 4B). Sample 04-AP-226 of Late Triassic (Norian) age was collected a considerable distance away from the above described sandstones (Figs. 2, 6). Its detrital zircon population is very similar to the above samples with Paleozoic peaks that are Cambro–Ordovician–Silurian and Carboniferous–Permian in age. There are very few zircons that are Silurian, Devonian and early Carboniferous (Fig. 4B). In addition, sample 04-AP-226 contains a few younger zircons that are 253, 259 and 268 Ma, all older than the host rocks, but too few to suggest this to be a big difference from paleo-Lena River derived samples without further work. Its main difference from previously collected samples is a higher proportion of Precambrian zircons compared to Paleozoic zircons (Fig. 4B) leading to low K–S P values when compared with the rest of the Verkhoyansk samples (Fig. 5).

Two samples from the inferred deeper water equivalents of the above continental and deltaic sandstones (the Kular-Nera Slate Belt) (samples R03-AP-25 and RA-3/5-01) (Figs. 2, 6), are similar to each other in terms of their range of Precambrian-age zircons (Fig. 4B), but their younger zircon age populations are different. The Precambrian populations contain relatively more 1.8–2.0 Ga zircons with most in a narrower 1.8–1.9 Ga range and no ages between these and 1.0 Ga. The Paleozoic age distribution of zircons has ages in the 500–550 Ma range, few in the 480–500 Ma age, and more ages in the Silurian and Devonian–early Carboniferous interval. Carboniferous–Permian zircons are similar in age to samples from continental to shelf settings, but constitute proportionally less of the total population of Paleozoic zircon (Fig. 4B). The most distinct aspect of the Kular–Nera detrital zircon population is the presence of a significant number of Triassic zircons in the age range from 235 to 240 Ma. As discussed by Prokopiev et al. (2008), sources in the Transbaikalian mountainous region, specifically the Carboniferous–Permian Angara–Vitim granitoid batholith and the Cambro–Ordovician magmatic arcs of the Altay–Sayan region are the most likely sources for zircons transported by the paleo Lena River and deposited along the Verkhoyansk margin in the Triassic. The Precambrian zircon age distribution in these samples is characteristic of rocks in the Siberian craton and Aldan shield, or could have been recycled from sediments derived from the erosion of those shield rocks. The Precambrian peaks are also those that characterize the present-day rivers that traverse Siberia (Safonova et al., 2010). Given the consistency of these ages in the paleo-Lena River derived Verkhoyansk sandstones through time (Prokopiev et al., 2008), the differences between the zircon populations of these sandstones and the zircon populations from sandstones of the offshore Slate Belt are likely significant (Fig. 5). In particular, there are no intermediate to silicic source rocks of Devonian–Early Carboniferous age on the Siberian platform. In fact, Devonian mafic volcanism associated with the formation of the Vilyui graben may have been accompanied by silicic (bimodal) eruptions, but would likely have been deeply buried by the Triassic and not a major source for zircons. The source of 235–240 Ma zircons in the Triassic rocks of the Slate Belt is also enigmatic as magmatic rocks of this age are limited to the younger accreted parts of the Verkhoyansk belt, the outboard Taigonos Peninsula (not shown on map) and Omolon terrane (Fig. 2) (Akinin and Kotlyar, 1997; Zhulanova et al., 2007). Middle Devonian to Early Carboniferous magmatic arc rocks are widespread in the Omolon terrane: volcanic rocks of the Kedon Formation as well as comagmatic granosyenite–porphyries and granodiorite–porphyries are present, and it is underlain by Precambrian basement rocks of Siberian affinities, thus of appropriate age to supply material to the deep water basin. The Koni–Murgal volcanic–plutonic belt located on the northwestern flank of the Okhotsk terrane (Fig. 2) has Triassic volcanic successions (Sosunov et al., 1982; Prokopiev et al., 2009). Co-author A.V. Prokopiev argues that paleocurrent measurements in deeper water Triassic slate belt rocks preclude an eastern source that these deeper water sediments

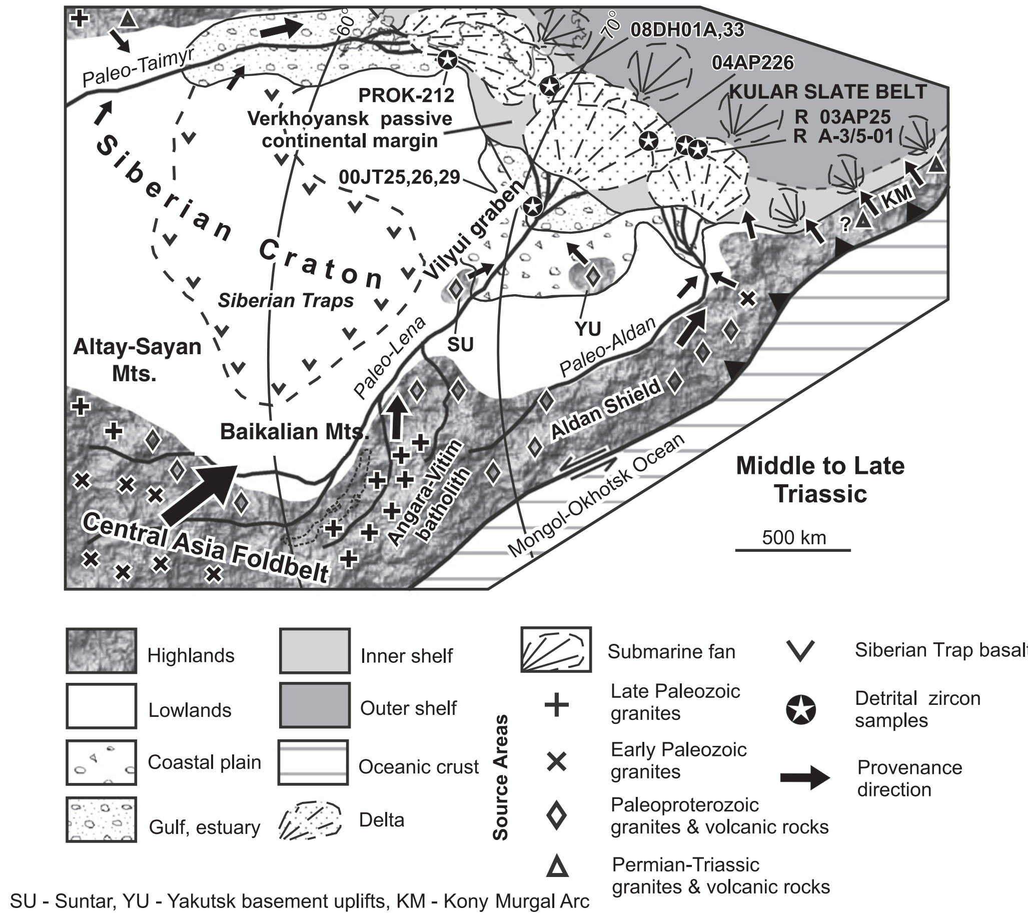

Fig. 6. Paleogeographic sketch illustrating the facies and provenance of samples from the Verkhoyansk margin.

must come from the west or from the south (Prokopiev and Tronin, 2004). Because these differences in detrital zircon populations suggest a different source area, perhaps from the Okhotsk terrane to the south, it is hoped that future work will better elucidate this part of North East Russia's paleogeography.

3.2. Northern Siberia paleo-Taimyr River System(s)

The closure of the Uralian seaway between Baltica and Siberia in the Early Permian (e.g. Nikishin et al., 1996) led to the collision of Siberia and Baltica–Laurentia, forming northern Pangea (Fig. 1). Widespread basaltic magmatism, beginning with the eruption of the Siberian traps and continuing into the Middle to Late Triassic (Nikishin et al., 2002; Torsvik and Andersen, 2002; Walderhaug et al., 2005; Reichow et al., 2009) took place across northern Siberia, the eastern flanks of the Uralian orogen, and in the Taimyr region (Fig. 2). As described by Nikishin et al. (2002), the west Siberia rift region, now entirely buried by sediments of the West Siberia Basin, was initially topographically elevated during the earlier stages of rifting. This is supported by arguments of Reichow et al. (2009) who showed that basalts were erupted across and likely covered a much greater region prior to rifting, faulting and subsidence of the West Siberian Basin. Thus it is likely that the west Siberia rift, as it developed, modified both sources of sediment and the location of river systems transporting clastic material seaward.

This second group of Triassic samples is distinguished in terms of its cumulative age probability plots (Fig. 4C) and higher P values in the K–S test (Fig. 5). The sources of the paleo-Lena River derived sandstones (discussed in the previous section) lay along the southern, active continental margin of Siberia (present-day coordinates) (Fig. 1). This orogenic collage wrapped around the western side of Siberia (present-day coordinates) and thus its component parts were ultimately involved in the joining together of Siberia, Kazakhstan and Baltica along the broader Uralian orogenic belt (Figs. 1, 2), now mostly covered by the deposits of the West Siberia Basin (Nikishin et al., 2002; Reichow et al., 2009) (Fig. 2). The detrital zircon signatures of the Triassic of the Verkhoyansk margin of Siberia therefore share similarities in terms of their igneous source terranes to those of units discussed in this section, especially in terms of their Paleozoic zircons (Figs. 4B,C and 5).

Sandstone interbedded with conglomerate at the base of the Upper Triassic (Rhaetian) Bulunkan Formation, deposited in a shallow marine or deltaic setting along the northeastern Siberian platform on the southeastern side of the Lena–Anabar basin adjacent to the Olenek basement uplift (sample PROK 212) (Figs. 2, 6) has a similar distribution of detrital zircon ages as do the shelf sandstones of the Verkhoyansk, with a significant number of Cambro–Ordovician zircons and late Carboniferous–Permian zircons and far fewer Silurian–Devonian–early Carboniferous zircons. It has two age peaks (~280 and ~301 Ma) that are also similar to Verkhoyansk samples, but sample PROK 212 has a greater proportion of Carboniferous versus Cambro–Ordovician zircons. Most importantly it includes the youngest peak at ~246 Ma (3 zircons, Appendix 3). Sources for sample PROK 212 are inferred to be rocks of the greater Uralian deformational belt characterized by magmatic arc systems that are ~300 Ma (Bea et al., 2002; Scarrow et al., 2002). The older Cambro–Ordovician zircons have the same probable source in the northern Urals as there are widespread rhyolites dated at 480–500 Ma (Kuzenkov et al., 2004; Soboleva et al., 2008a,b). There are also intermediate to silicic tuffs, sills and volcanic strata in the Severnaya Zemlya archipelago

(Fig. 2) dated by Lorenz et al. (2007) as ~490–475 Ma (U–Pb, zircon). Triassic zircons are common in all subsequently discussed samples and their sources are considered in a following section.

Triassic strata mapped as Ladinian in age (Oleshko, 1981) and deposited in a marine deltaic setting were sampled from a position considerably more internal to the Verkhoyansk orogen (Samples 08DH1A and 33) (Figs. 2, 6). Similar to the sample discussed above, these two samples exhibit zircon age peaks at 496 and 503 Ma in the 480–505 Ma age range and at ~300 Ma in the 295 to 308 Ma age range (Appendix 3). In addition, they contain up to 15% Triassic zircons with age peaks at ~238 Ma (08DH01A) and ~236 Ma (08DH33) (Appendix 3) and up to 10% Permian zircons with an age peak at ~264 and 268 Ma. As such, these two samples are most similar to the detrital zircon populations of samples from B. Lyakhov Island, New Siberian Islands, and Chukotka (discussed next) but were deposited in a shelfal, not basinal, environment. The sources for the younger parts of the zircon population are discussed in context with the New Siberian Islands and Chukotka samples.

Sandstones from the New Siberian Islands, Chukotka and Wrangel Island are classed within the paleo-Taimyr River System group of samples. Most of these strata were deposited in a deep-water environment by gravity flow processes (e.g. Miller et al., 2006; Kuzmichev and Goldyrev, 2007; Tuchkova et al., 2007; Miller et al., 2010) and are much more complexly deformed and metamorphosed than Triassic strata of the Verkhoyansk fold belt (Fig. 2). The overall similarity of the detrital zircon populations of this set of samples provide a strong argument for similar sources, possibly delivered by one or more main river systems draining that source region (Figs. 4C, 5). In particular, previously published data from Chukotka (samples CH3.1B, CH2.6 and CH26.5) are very similar to sample KUZ146-1 from Bolshoi Lyakhov Island, New Siberian Islands, dated by SHRIMP-RG (analytical methods and data table in Appendix 2). Sandstones from these two regions, now ~1300 km apart, have similar amounts of 250–265 Ma, ~300 Ma and Cambro–Ordovician zircons. The presence of greater amounts of Devonian zircons and greater amounts of latest Permian to Permo–Triassic zircons distinguishes this group of samples from the Triassic of the Verkhoyansk (Figs. 4, 5). In addition, the B. Lyakhov and Chukotka samples have Precambrian zircon populations with more ages in the 500–1000 Ma range and also in the 1000–1800 Ma range compared to the virtual lack of these ages in the Verkhoyansk samples (Fig. 4B and C). Sample KUZ146-1 from Bolshoi Lyakhov Island was collected from the deformed Burus-Tas Formation described in detail by Kuzmichev et al. (2006). Geologic mapping and sampling prior to Kuzmichev et al. (2006) study assigned the Burus-Tas to the Permo–Triassic (Vol'nov et al., 1999). Kuzmichev et al.'s (2006) study concluded that the Burus-Tas was part of a Jurassic to Cretaceous clastic wedge shed from the south during the accretion of an arc to the Siberian margin. However, a detailed study of better exposed and dated Jura-Cretaceous siliciclastic strata on Stolbovoi Island (New Siberian Islands) discussed in Miller et al. (2008), together with the analyses of detrital zircons from these strata, clearly showed that there were significant differences between the zircon populations of Triassic versus Jura-Cretaceous deposits. These comparisons allow us to conclude that sample KUZ146-1 is Triassic and not Jurassic in age as previously described by Kuzmichev et al. (2006).

To provide greater insight to the sources represented by this second group of sandstones with very similar detrital zircon populations (Figs. 4C, 5), we hand-picked euhedral zircon populations (e.g. Fig. 3) from representative splits of sample KUZ146-1 and KUZ145-8 from Bolshoi Lyakhov Island (New Siberian Islands), from samples ELM03 CH2.6 (Chukotka) and C145735 (Wrangel Island). Fig. 7 illustrates the euhedral zircon populations we dated and their range of ages. Analytical methods and data tables for the SHRIMP-RG analyses of these zircons are found in Appendix 2. In both B. Lyakhov Island (New Siberian Islands) and Chukotka–Wrangel samples, the ages of euhedral zircons represent both the very youngest part of the populations analyzed with the LA-ICP-MS method and are also representative of the Paleozoic peaks obtained during the random walk dating of dump-mounted zircon (Figs. 3, 7). On B. Lyakov Island (New Siberian Islands), the youngest U–Pb SHRIMP ages on zircon from two Triassic samples were 244.5 ± 2.6, 247.2 ± 5, 250.5 ± 2.5 and 258.1 ± 2.0 Ma (1 sigma errors). Euhedral zircons in the 260–400 Ma age range are also represented as well as those ranging in age from ~424 to 515 Ma (Fig. 7). Only one Precambrian zircon is represented in the hand-picked, euhedral zircon suite. This data suggests that the source region(s) for the Triassic sandstone turbidites of B. Lyakhov Island (New Siberian Islands) included Paleozoic igneous rocks with a range of ages spanning the Cambrian to the Permo–Triassic, all likely eroding for the first time. The Precambrian zircon population as a whole in these samples is more likely to have been recycled from sedimentary/metasedimentary sources. Dating of euhedral hand-picked zircons from Chukotka (Fig. 7) and Wrangel Island samples yielded similar results. The youngest zircons from the Chukotka sample yielded ages of 233 ± 2.1, 235.8 ± 2.6 and 239.7 ± 2.1 Ma and the sample from Wrangel Island, 266 ± 2.9. Permo–Triassic to Carboniferous zircons in these two samples are likely first cycle as are the Devonian, Ordovician and Silurian zircons. Only three Precambrian euhedral zircons were dated and no euhedral zircons were dated in the 500–600 and 700–900 age range, despite the fact that zircons of this age are well represented in the LA-ICP-MS analyses of these samples (Fig. 7), suggesting that zircons in these age ranges may also have a recycled origin. The difference in the youngest age component of zircons is likely a reflection of different depositional ages, which are only poorly known in these deformed Triassic sequences (Miller et al., 2006, 2010).

The Late Permian sequence and the base of the Triassic stratigraphic section are characterized by abundant gabbro/diabase dikes and sills (e.g. Gelman, 1963; Miller et al., 2006; Kuzmichev and Goldyrev, 2007; Kuzmichev and Pease, 2007). They have been dated by the U–Pb method in only two places, a great distance from each other, on B. Lyakhov Island (New Siberian Islands) as 252 ± 2 by Kuzmichev and Pease (2007) and in eastern Chukotka as 252 ± 2 Ma by Ledneva et al. (2011) (Fig. 2). Kuzmichev and Pease (2007) present geochemical data that link the mafic magmatism on B. Lyakhov Island (New Siberian Islands) to the initiation of Siberian trap magmatism, thereby physically linking the New Siberian Islands to Siberia and Taimyr prior to rifting that led to the formation of the Laptev Sea and Eurasia Basin (Fig. 2). Ledneva et al. (2011) suggest the same for the mafic magmatism studied in easternmost Chukotka (Fig. 2). These relations and ages provide a strong rational for correlating and linking Triassic depositional systems across Arctic Russia east of the Taimyr (Fig. 2), an argument which is greatly strengthened here by the observed similarities in the detrital zircons suites of Triassic strata.

An important aspect of the detrital zircon populations from both B. Lyakhov Island of the New Siberian Islands and Chukotka is the fact that they include Triassic age zircons. At least in the northernmost Urals, where closure of the Uralian seaway was over by the early Permian, there are no mapped plutonic belts with ages younger than about 300 Ma. Further south in the Urals, post-collisional magmatic–granite complexes yield ages as young as about 250 Ma (Bea et al., 2002) and may represent source regions for these zircons. Mafic and more limited felsic magmatism continued into the Triassic in the Taimyr region (Vernikovsky et al., 1995, 1998, 2003; Walderhaug et al., 2005). Basalts in the southern Taimyr have been studied and dated as 227–229 Ma (40Ar/39Ar) by Walderhaug et al. (2005) and A-type granites and syenites as 241–249 Ma (U–Pb, zircon) (Vernikovsky et al., 2003). The Novaya Zemlya loop (Fig. 2) formed into the Late Triassic (Scott et al., 2010) and the Kara Sea is known to include Permo–Triassic to Triassic rifts likely associated with rift-related magmatism (Nikishin et al., 2011). Large mafic igneous provinces, particularly those initiated beneath continental crust, usually produce a minor component of silicic magma that erupts in explosive fashion (e.g. Pankhurst et al., 2010).

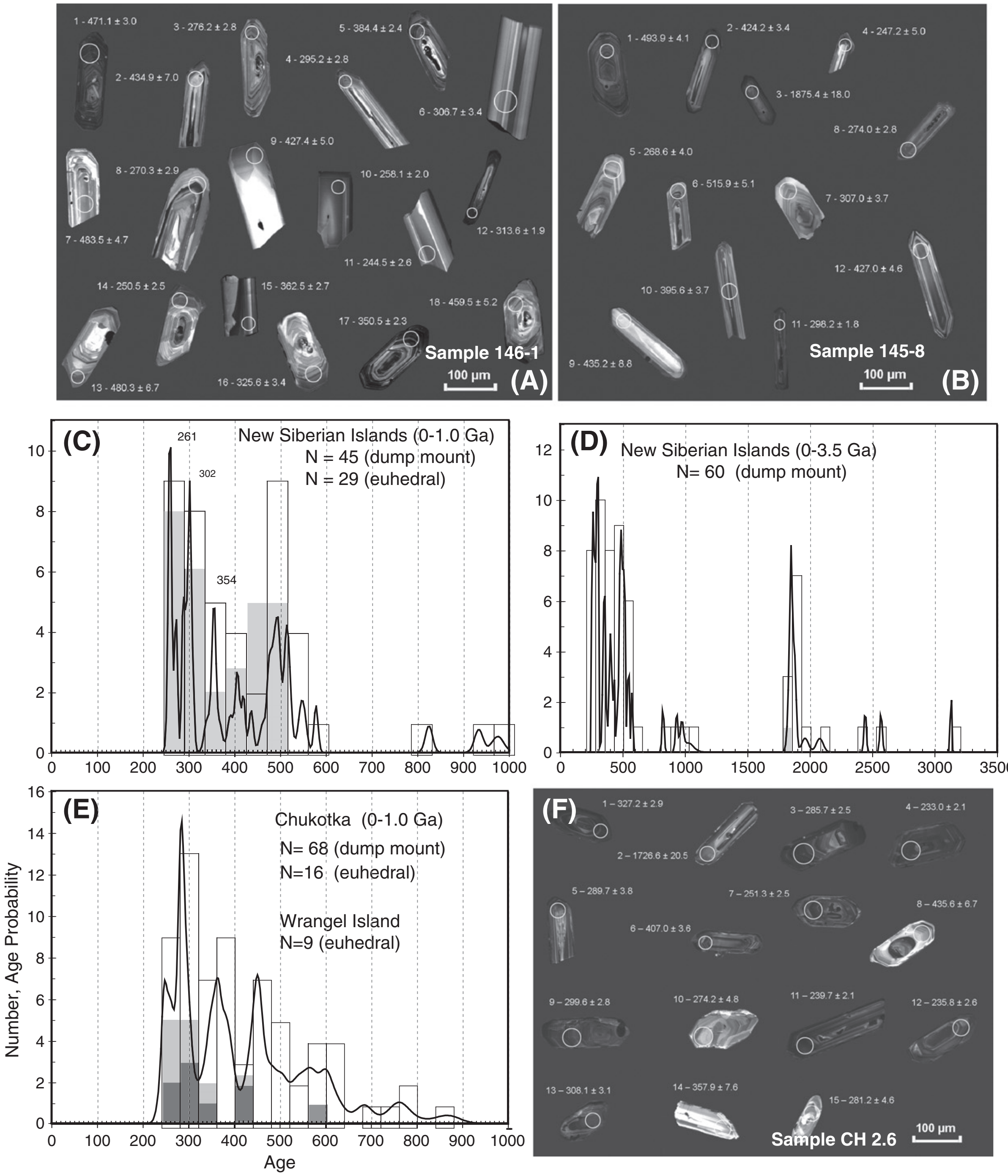

Fig. 7. A, B. Cathodoluminescent images and SHRIMP-RG spot ages of hand-picked euhedral zircons from detrital populations of sandstone samples 146-1 and 145-8 from Lyakhov Island (New Siberian Islands). C, D. Data from these euhedral zircons (gray histogram) are compared with SHRIMP-RG ages collected from dump mounted, random walk dating of sample 146-1 (Fig. 3) (as shown by the relative age probability plot and white histogram). Hand-picked population is shown by dark gray histogram. E. Less that 1.0 Ga ages from sample ELM03-CH2.6 from Chukotka dated by LA-ICP-MS (Miller et al., 2006) (as shown by the relative age probability plot and white histogram) together with ages of hand-picked euhedral zircons from the same sample (N = 16) (light gray histogram) and from sample W145737 from Wrangel Island (dark gray histogram). F. CL images of dated zircons from CH2.6 (Wrangel Island zircons are not shown). SHRIMP analytical techniques and data tables for these samples are in Appendix 2. For discussion, see text.

We hypothesize that this igneous province, despite most of it now being covered by younger sediments, may have been the closest and most reasonable source(s) for Triassic age zircons in basinal Triassic rift deposits. Their ~260 to 235 observed age range could reflect the broader age of both mafic and lesser associated felsic magmatism through this interval of time.

Zircon populations from Triassic strata on Wrangel Island and from the Lisburne Hills, Alaska (Figs. 2 and 6) are described in detail by Miller et al. (2006, 2010). The unfossiliferous and monotonous nature of Triassic gravity flow deposits on Wrangel Island, coupled with their internal deformation, compromise an accurate picture of their stratigraphy and thicknesses. However, they are distinguished from similar Triassic sequences in Chukotka by the lack of diabase dikes and sills and, in general, a higher sand to shale ratio (Miller et al., 2006; Tuchkova et al., 2007). The Triassic sequence of Wrangel Island represents a section deposited more proximal to a continental margin as compared to the Triassic of Chukotka which lay in a more distal basinal setting during deposition. The Triassic of Wrangel

Island, like the Triassic of Chukotka, was deposited in a basin or series of basins developed across a Late Paleozoic carbonate platform that was rifted apart and foundered beginning in the latest Permian (Miller et al., 2006, 2010). The underlying, mostly Carboniferous, succession was deposited on Neoproterozoic basement and contains Baltica-affinity detrital zircon populations (Miller et al., 2010). An important difference in the detrital zircon populations of the Chukotka samples compared to B. Lyakhov Island of the New Siberian Islands is that they contain a greater percent of Neoproterozoic ~550 to 750 Ma zircons. This age range of zircons, although likely recycled, is more characteristic of Paleozoic sediments and their underlying basement, not only on Wrangel Island, but in the northern part of the Taimyr, Severnaya Zemlya and the Kara Sea block (Lorenz et al., 2008; Pease and Scott, 2009) rather than Siberia, where there are no known sources of this age (e.g. compare sample curves in Fig. 4B and C).

The Triassic of the Lisburne Hills, Alaska (Miller et al., 2006), represents an unusual, 5 m thick interval of medium-grained shelf-facies sandstone of the Triassic Otuk Formation which forms part of the well-known North Slope sequence of northern Alaska. Based on subsurface data, it has been shown that Triassic deposits of the North Slope sequence (which includes the Lisburne Hills sequence) terminate against or depositionally onlap a basement high, the Chukchi High, which likely served as a paleogeographic high or continental region in this part of the Arctic during the Triassic (e.g. Sherwood et al., 2002). Given that the Triassic of the Lisburne Hills is separated from the Triassic of Chukotka and Wrangel Island by this high and is of different facies (shelf versus basinal), it is remarkable that their detrital zircon populations suggest derivation from nearly identical sources (Figs. 4C,5). The Triassic from both regions have similar Ordovician–Silurian populations with peaks at ~440 Ma (~439 Ma Wrangel and ~442 Ma Lisburne). They both have a population of Carboniferous zircons, which is relatively greater in the Lisburne samples versus the Wrangel samples, with age peaks at about ~300 Ma (~317 Ma Wrangel, 296 Ma Lisburne). Permo–Triassic zircons are also present (relatively more in the Lisburne than Wrangel samples) as are small populations of Triassic zircons ranging from ~235–215 Ma (Appendix 3). In terms of Precambrian zircon populations, the striking lack of ~1100–1800 zircons characterizing B. Lyakhov Island of the New Siberian Islands and all Siberian samples is clearly not the case in the Chukotka, Wrangel and Lisburne samples. These latter samples have variable minor amounts of zircons in this age range. Although there are many similarities between the detrital zircon populations of B. Lyakhov Island, Chukotka, Wrangel and Lisburne Hills Triassic sediments (Figs. 4 and 5), it is also clear that there are changes in the age distribution of zircons from west to east that may be important in terms of furthering our understanding of the regional setting and location of the more detailed depositional systems that delivered clastic material to this system of Triassic basins. For example, there is a shift in the age of early Paleozoic peaks in the zircon populations from ~490–500 Ma (Cambro–Ordovician) in Siberia and the B. Lyakhov Island samples to ~440–450 Ma (Ordovician–Silurian) on Wrangel Island and in the Lisburne Hills. The older age peak is common in all Triassic strata tied closely with Siberia but the younger age peak 440–450 is typical of sources originating in the Caledonian orogenic belt between Baltica from Laurentia (Figs. 1 and 2; Miller et al., 2006, 2010). Otherwise all of these Triassic strata share upper Paleozoic zircon populations of Devonian and Carboniferous-Permian age, common in batholithic belts of the northern Ural Mountains (Bea et al., 2002). They also contain a significant amount of Late Permian to Permo–Triassic 260–250 Ma and lesser amounts of Triassic age zircon. This younger part of the zircon population is not characteristic of the Triassic of the Verkhoyansk margin which has very few zircons younger than ~300 Ma, or the Polar Urals, where youngest igneous ages are mostly ~300 Ma. A possible source for these Permo–Triassic zircons is, as suggested above, silicic eruptions associated with large mafic igneous provinces in Siberia, Taimyr and the Kara Sea/Novaya Zemlya region, and the syenitic intrusions of latest Permian to Early Triassic age in the Taimyr (Vernikovsky et al., 2003). Alternative sources might be the geographically more distant parts of the Urals and/or their equivalents now mostly buried under the West Siberia Basin. During the closure of the Uralian Sea and post-dating it, suites of granitoids were intruded that are as young as the late Permian (260–250 Ma) and are associated with deep-seated migmatitic complexes (Bea et al., 2002). Thus the erosional and/or tectonic unroofing of these rocks constitute an additional, but more distant, potential source for Permo–Triassic age zircons, which are a characteristic shared between Triassic strata of B. Lyakhov Island of the New Siberian Islands, Chukotka, Wrangel and Lisburne Hills (Figs. 4, 5).

3.3. North America (Laurentian) River systems

We contrast the data sets from the Russian and westernmost Alaskan Arctic discussed above with data from the Triassic of the northernmost Cordillera, exposed near the border of Alaska and Canada in the Yukon (Beranek et al., 2010) (Fig. 2). Here, Carboniferous to Triassic sediments were deposited along a west-facing continental margin in shelfal environments and were derived from the craton that lay to the north and east (Fig. 2; Beranek et al., 2010). The detrital zircon populations of the Triassic strata in the Yukon region are distinctly different from any of the Triassic data discussed so far in that the youngest ages represented are far older than the age of enclosing sediments (Samples JL2, OG3, OG4, SL, HL, TF; Fig. 4D). The youngest parts of the zircon population include limited 360–390 Ma Devonian zircons derived from plutonic rocks of this age which occur across Arctic Alaska and Canada and more abundant Ordovician-Silurian (~410–480 Ma) zircon derived from Caledonian sources. The samples contain variable amounts of Neoproterozoic zircons between 500 and 700 Ma and then a variable Precambrian population with ages between 900 and 2000 Ma and lesser 2300–3000 Ma zircons, which are typical Grenville and Precambrian Shield source ages (Fig. 4D). In terms of their K–S P values, this set of samples is similar to each other and easy to differentiate from all samples previously discussed (Figs. 4, 5). These differences form a robust basis with which to postulate a third set of river systems that transected Laurentia carrying debris derived from highlands in what are the North Atlantic and Arctic regions, or the trans-Laurentia River systems (Figs. 4 and 5).

3.4. The Alaska and Canadian Arctic

There is only one published detrital zircon suite from Triassic sediments of Arctic Alaska (Fig. 2) and, as such, its comparison to the data sets discussed above remains tentative. The Triassic Ivishak Formation in the Sadlerochit Mountains, northeastern Alaska, was deposited in a shallow marine deltaic environment and derived from a northern source terrane (Mariani, 1987). Sample 96DH102 (Miller et al., 2006) has a more limited range of zircon ages compared to other samples discussed here suggesting that it may have been locally sourced (Figs. 2, 4E, 5, 8). The detrital zircon population is dominated by Cambrian–Neoproterozoic zircons (peaks at ~530 and 550 Ma; Fig. 4E) and a lesser amount of Cambro–Ordovician zircons (~440–460 Ma; Fig. 4E, Appendix 3). This distribution of ages is unlike the North America-derived Triassic of the Yukon (Beranek et al., 2010) which contains abundant Ordovician–Silurian and older Precambrian zircons (compare curves in Fig. 4D and E). Sample 96DH102 also lacks the Permo–Triassic, Permo–Carboniferous, and Devonian ages that are characteristic of the paleo-Taimyr River samples (Fig. 4C). Its population is clearly distinguished (unique) on the basis of its cumulative age probability curve and comparison to other samples using K–S P values (Figs. 4E and 5).

Canada's Sverdrup Basin (Fig. 2) was a broad basin situated in Arctic Canada that, in the Triassic, had both southern source regions (cratonic North America and Greenland) and northern source regions that are removed by subsequent rifting (Embry, 1991, 1992; Miller et al., 2006;

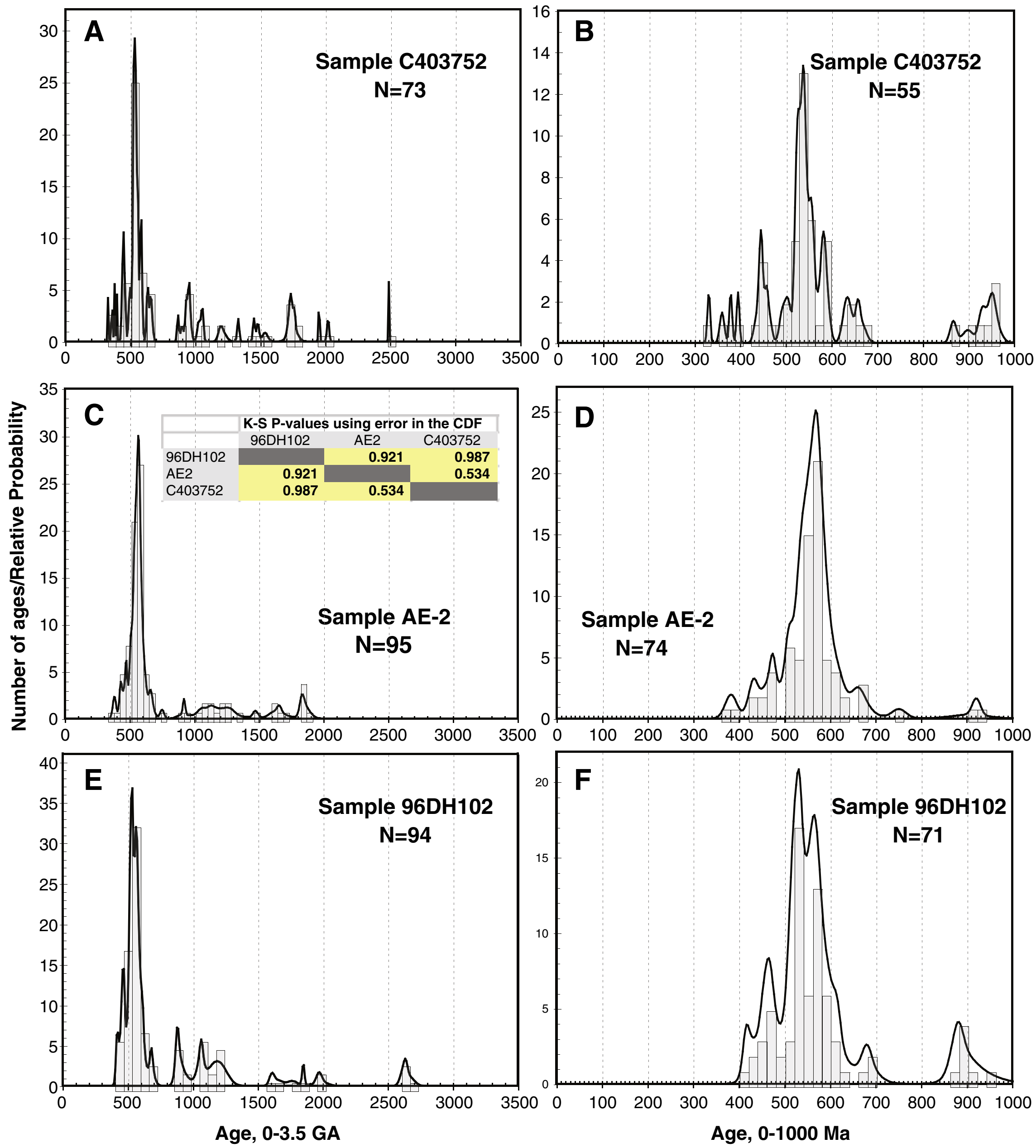

Fig. 8. Comparison of data from Omma et al.'s (2011) sample C403752 (Sverdrup Basin) (A and B) to Miller et al.'s (2006) samples AE-2 (Sverdrup Basin) (C and D) and 96DH102 (northeastern Alaska) (E and F). For discussion, see text.

Embry, 2011; Omma et al., 2011). The source region removed by rifting and formation of the Canada Basin (Fig. 2) has been called "Crockerland" (Embry, 1991, 1992). The two Triassic samples from the Sverdrup Basin discussed in Miller et al. (2006) were given to us by A. Embry and represent sandstone derived from the southerly and northerly (Crockerland) source regions. Sample AE-1 from the Bjorne Formation, central Ellesmere Island, was sourced from the east and from the south (Embry, 1991). The Bjorne Formation contains almost entirely Precambrian zircons (only 9 zircons younger than 1 Ga) that range from 1 Ga to 2.1 Ga with a notable lack of zircons in the 1.4 to 1.6 Ga range, and lesser zircons in the 2.3–3.4 Ga range (Figs. 4D, 5). The detrital zircon suite in this sample is similar to Beranek et al.'s (2010) samples of North American derivation but his samples have more zircon in the 1.4–1.6 Ga range and relatively more Neoproterozoic and Caledonian ages, likely reflecting a broader range of source regions, including parts of the Caledonides in Arctic Canada (Fig. 2). We group sample AE-1 with the North American samples in our comparison (Figs. 4D, 5).

Sample AE-2 is from the Middle Triassic (Carnian) Pat Bay Formation, a shallow marine sandstone inferred (based on thickness and facies) to have been derived from the *northern* margin of the Sverdrup Basin or from Crockerland (Embry, 1991, 1992, 2011; Miller et al., 2006). A limited range of ages is seen in sample AE-2 that is similar to sample 96DH102 from the Ivishak of northeastern Alaska (Figs. 4, 5). Statistically, these two samples are similar to each other with K–S test P values greater than 0.9 (Fig. 5) and significantly different from any of the other samples discussed here.

Sample C403752 analyzed by Omma et al. (2011) is the same as sample AE-2 analyzed by Miller et al. (2006), both provided by A. Embry of the Canadian Geological Survey from a single large sample of the Triassic (Carnian–earliest Norian) Pat Bay Formation collected by him on northern Axel Heiberg Island. Omma et al. (2011) revised the stratigraphic assignment of this sample to the Jurassic (Pliensbachian) uppermost Heiberg Formation based on a comparison of its heavy mineral suite to unpublished heavy mineral data sets from the Heiberg Formation.

Embry maintains that the sample was collected from the Pat Bay Formation and not the Heiberg Formation (Embry, pers comm., 2012). Both Miller et al. (2006) and Omma et al. (2011) point out the restricted Late Neoproterozoic–Cambrian age igneous source for this sandstone and suggest a northern derivation, most likely from Timanian orogenic belt rocks in northern Baltica.

Omma et al. (2011) provide additional U–Pb detrital zircon ages for four Triassic and Jurassic samples from the Sverdrup Basin. The data are quite different from sample to sample, indicating changing source regions during this time-span. We do not include these data in our comparison because the number of U–Pb ages reported for each sample is in some cases significantly less than 100 and both the variation in stratigraphic ages and the differences in detrital zircon ages reported made it unreasonable to group data from more than one sample together. Three of these samples, however, clearly contain large populations of Carboniferous–Permian (~280 Ma) zircons as well as Triassic zircons that range from ~235 to 216 Ma (Omma et al., 2011). These new data are highly significant in that they suggest that sediment transport existed between the Taimyr–Novaya Zemlya–Ural orogenic belt, the edge of the Barents Shelf and Canada's Sverdrup Basin in the Triassic–Jurassic (Omma et al., 2011). Once opening of the Eurasian Basin is restored, the northern and eastern edges of the Sverdrup Basin lie adjacent to the Barents Shelf near Svalbard (Omma et al., 2011) (Figs. 1 and 2).

3.5. Svalbard and Franz Josef Archipelagos

Svalbard exposes a gently tilted stratigraphic section of the Barents Shelf sedimentary succession (Fig. 2). This pre-Devonian to Paleocene section was tilted and uplifted as a result of rifting along the nascent margin of the Eurasia Basin of the Arctic (Henriksen et al., 2011)(Figs. 1, 2). The Triassic part of the succession consists of sandstone, siltstone and siliceous mudstone (e.g. Hoy and Lundschien, 2011). Preliminary detrital zircon studies by LA-ICP-MS report a change in provenance in the Triassic (Bue et al., 2012). The lower and middle parts of the Triassic section (the Vardebukta and Bravaisberget Formations) have detrital zircon age peaks at 400–480 Ma, 900–1500 Ma, 1.6–2.1 and 2.6–2.9 Ga, with no zircons younger than 400 Ma. Late Triassic sandstones (Wilhelmoya and De Geerdalen Formations), in contrast, have a significant amount of zircons that are 200–700 Ma, 900–1100 Ma, 1.2–2.0 and 2.5–3.2 Ga. The Ordovician–Silurian zircons in the lower and middle parts of the Triassic together with the lack of upper Paleozoic zircons suggest sources in the Caledonian orogenic belt, either locally (basement of Svalbard) or from the Greenland Caledonides. Late Paleozoic zircons in the younger part of the Triassic suggest that there was a significant change in source region with sediment derived from the greater Novaya Zemlya–Taimyr–Ural region (Bue et al., 2012).

Detrital zircon populations from four Triassic samples from Franz Josef Land (Pease et al., 2007) indicate upper Paleozoic Uralian sources as well with age peaks at ~250, 290, 330 and 420–460 Ma; older (500–2800) sources are also present but vary from sample to sample (Pease, 2011, 2007). All ages are consistent with derivation from local Eurasian sources (Pease et al., 2007).

4. Summary and conclusions: implications for paleogeography and plate tectonic reconstructions

Fig. 9 presents a summary of the data discussed above, where all data from each of the three major inferred river systems were grouped to compare them more broadly to each other. The key distinctive features of these different groups of data are as follows: The paleo-Lena with Siberian sources is distinguished by the almost total lack of zircons in the age range 550 Ma to 1.8 Ga. The paleo-Taimyr, with Uralian sources, is characterized by large percentages of upper Paleozoic zircons. The trans-Laurentia river system(s) is characterized by a conspicuous lack of upper Paleozoic zircons. This comparison also points out the unique nature of source areas (Crockerland) that fed clastic material into the northern Sverdrup Basin. These differences describe important fundamental features of the plate tectonic setting and Triassic paleogeography of northwestern Pangea (Fig. 1). As the base map for Fig. 1, we used Lawver et al.'s (2002) plate reconstruction for the Triassic, spanning from ~240 to 210 Ma, and on this map, illustrate events as old as latest Permian. At this time, northwestern Pangea's ocean margin faced a paleo-Pacific Ocean to the north and west (Lawver et al., 2002) (Fig. 1). The sediment transport systems discussed above are shown schematically as hypothetical river systems draining geographically extensive but otherwise unique source regions at that time (Fig. 1). Although schematic, the general locations and geometry of these river systems make the overall point that Triassic sediments were derived from separate parts of northern and western Pangea and that these sources can be identified based on detrital zircon populations (Fig. 9). The data discussed in this paper also suggests that these source regions were related to unique paleogeographic elements that were tectonic in origin and that there may have been major drainage divides between the trans-Laurentia river systems and the paleo-Taimyr river systems. Fig. 1 also emphasizes that the relatively simple rifted and passive margin paleogeography and inferred structural and stratal continuity of sediments shed into the paleo-Pacific margin of northwestern Pangea stands in stark contrasts to the complex geology of the Arctic today (Harrison et al., 2008; Fig. 2), emphasizing the importance and extent of both compressional and extensional orogenic events, rifting and plate motions that must be restored in order to better appreciate the original features of Arctic paleogeography in the Triassic.

Our understanding of the pre-rift location of the Russian part of the Arctic Alaska-Chukotka microplate (Fig. 1) is better understood as a result of the analysis of data presented here. A preliminary analysis of detrital zircon suites from the Chukotka part of the microplate (Miller et al., 2006) suggested that it restored to Siberia rather than Canada (compare Lawver et al., 2002; Miller et al., 2006). The data discussed here further support and expand on this preliminary conclusion. In particular, the high degree of similarity between detrital zircon suites from B. Lyakhov Island of the New Siberian Islands and those of Chukotka, coupled with the geochronology and geochemistry of mafic lavas intercalated with these sequences (Kuzmichev and Pease, 2007; Ledneva et al., 2011) now strengthens the ties of Chukotka to the New Siberian Islands, suggesting Chukotka restores to a position closer to Taimyr after closure of the North Atlantic, removal of stretching in the Laptev Sea, and restoration of rifting in the Amerasia Basin (Figs. 1, 2). It should be noted that during Triassic time, most or all of the now on-land Chukotka part of the Arctic Alaska-Chukotka "microplate" as portrayed by Lawver et al. (2002) actually lay in deep water, rift basin setting (Fig. 1). In other words, at least part of Chukotka was not strictly "continental" in the Triassic because deep-water Triassic deposits overlie rifted and foundered Paleozoic shelf strata and their underlying Neoproterozoic crystalline basement across Chukotka (Miller et al., 2010, 2011). Thus Chukotka was likely underlain by only thinned continental crust in the Triassic. Despite its inferred offshore location in the Triassic (Fig. 1), it had sedimentary ties with at least the westernmost part of northern Alaska: the detrital zircon populations of Triassic sandstones in the Lisburne Hills section of Arctic Alaska are very similar to those of Triassic strata on Wrangel Island, suggesting the same (paleo-Taimyr and/or Ural region) sources. Upper Paleozoic strata that underlie the Triassic in both the North Slope section and on Wrangel Island have similar (Baltica-proximal) signatures (Miller et al., 2010, 2011) but lack the thick Triassic clastic successions typical of Chukotka. These relations link the Chukotka part of the Arctic Alaska–Chukotka microplate to westernmost Alaska and suggest that the pre-rift configuration of Chukotka and westernmost Alaska was adjacent to the Lomonosov Ridge and Barents shelf, in a position now presently

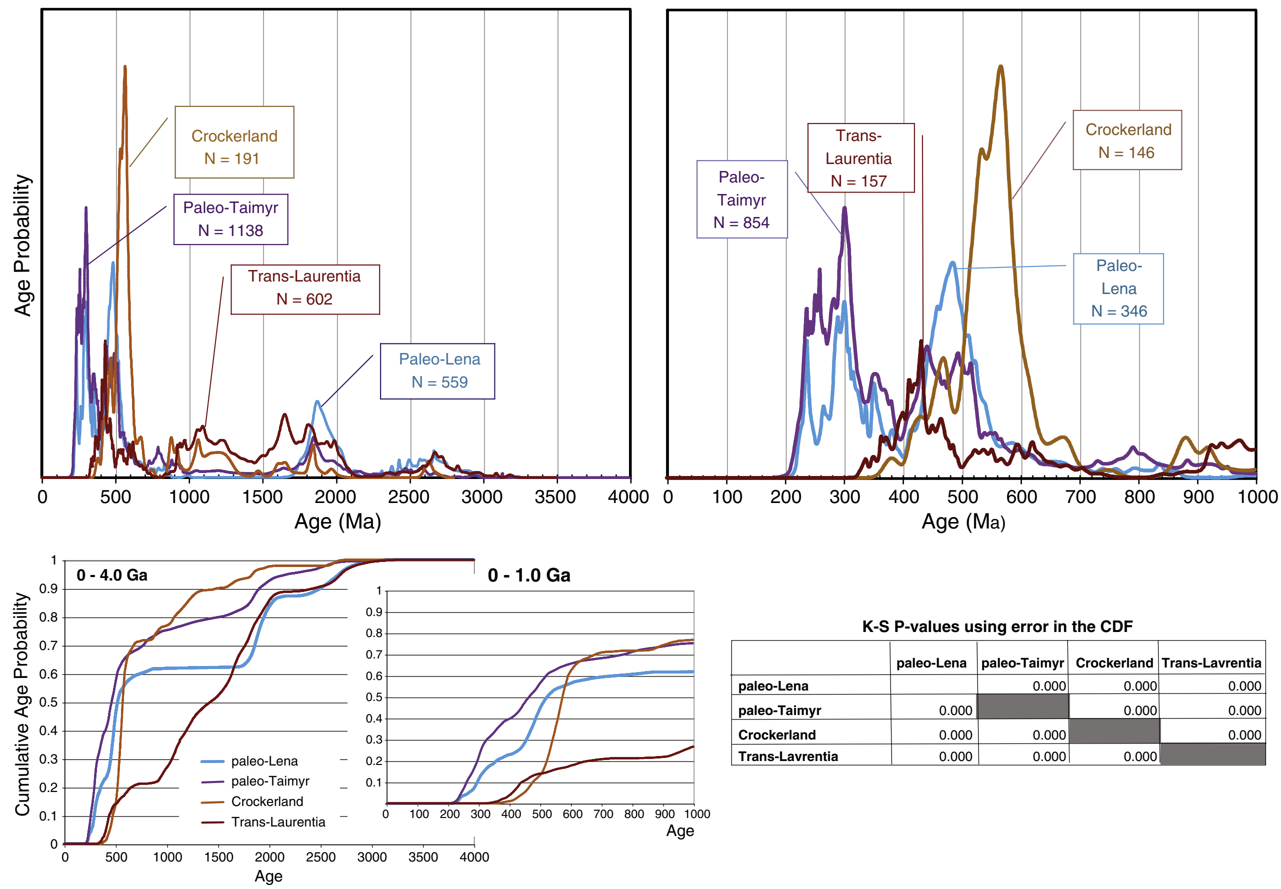

	paleo-Lena	paleo-Taimyr	Crockerland	Trans-Lavrentia
paleo-Lena		0.000	0.000	0.000
paleo-Taimyr	0.000		0.000	0.000
Crockerland	0.000	0.000		0.000
Trans-Lavrentia	0.000	0.000	0.000	

Fig. 9. Comparison of combined data sets from the three major inferred Triassic depositional systems and Crockerland based on age probability plots (top) and cumulative age probability plots and P values resulting from K–S test (bottom). For discussion, see text.

east of the Caledonides and west of the Polar Urals (Miller et al., 2010) (Fig. 1).

Acknowledgements

We thank Exxon-Mobil, Shell Development and British Petroleum whose interest in the Arctic over the years led to the collection and analysis of many of the samples described here. A part of the project resulted from a collaborative study and visit by Soloviev to Stanford University funded by the Blaustein visiting scholar program of the School of Earth Sciences. We thank Dr. J. Wooden for his guidance and help with the SHRIMP-RG analyses and A. Strickland for SHRIMP-RG analysis of detrital zircons from sample KUZ148-5. Acknowledgment is made to the donors of the American Chemical Society Petroleum Research Fund for support of part of this research. PRF Award 45432-AC8 to Elizabeth Miller supported logistics and fieldwork on Wrangel Island and subsequent analytical work discussed in this paper. National Science Foundation Award EAR-0948673 to Miller and CRDF RUG1-2994-MA-11 to Akinin and Miller funded additional fieldwork and analyses presented here. Logistics and fieldwork to the Kular Region were partially supported by RFBR 07-05-00743 to Prokopiev. These latter awards have supported equal efforts towards dating magmatic rocks that served as source regions for Arctic sediments. NSF-EAR 0732436 supported the Arizona LaserChron Center. We thank William Nielsen for helping us draft the paleogeographic maps.

Appendix A. Supplementary data

Supplementary data associated with this article can be found in the online version, at http://dx.doi.org/10.1016/j.gr.2012.08.015. These data include Google maps of the most important areas described in this article.

References

Akinin, V.V., Kotlyar, I.N., 1997. GEOCHRON — computer database of isotope dating of minerals, rocks and ores of northeast Russia. Magmatism and mineralization of northeast Russia. SVKNII DVO RAN, Magadan, pp. 313–318 (in Russian).

Babinski, M., Boggiani, P.C., Tindade, R.I.F., Fanning, C.M., 2012. Detrital zircon ages and geochronological constraints on the Neoproterozoic Puga diamictites and associated BIFs in the southern Paraguay Belt, Brazil. Gondwana Research. http://dx.doi.org/10.1016/j.gr.2012.06.011.

Bea, F., Fershtater, G.B., Montero, R., 2002. Granitoids of the Uralides: implications for the evolution of the orogen. In: Brown, D., Juhlin, C., Puchkov, V. (Eds.), Mountain Building in the Uralides: Pangea to the present: American Geophysical Union Geophysical Monograph, 132, pp. 211–232.

Beranek, L.P., Mortensen, J.K., Orchard, M.J., Ullrich, T., 2010. Provenance of North American Triassic strata from west-central and southeastern Yukon: correlations with coeval strata in the Western Canada Sedimentary Basin and Canadian Arctic Islands. Canadian Journal Earth Sciences 47, 53–73.

Bue, E.P., Andresen, A., Andersen, T., Solbakken, R.T., 2012. Provenance of Mesozoic sediments from Svalbard based on LA- MC-ICPMS analyses of clastic zircons: Preliminaryresults. ftp://ftp.ngu.no/pub/NGF_Wintermeeting/Til%20Hans%20Arne/EBCE/EBCE3+6/PGE3O_Bue_Edina_Pozer.pdf.

Colpron, M., Nelson, J., 2011. A Paleozoic NW passage and the Timanian, Caledonian and Uralian connections of some exotic terranes in the North American Cordillera. In: Spencer, A.M., Embry, A.F., Gautier, D.L., Stoupakova, A.V., Sørensen, K. (Eds.), Arctic Petroleum Geology: Geological Society London Memoir, 35, pp. 463–484. http://dx.doi.org/10.1144/M35.31 (0435-4052/11).

Condie, K.C., Belousova, E., Griffin, W.L., Sircombe, K.N., 2009. Granitoid events in space and time: constraints from igneous and detrital zircon age spectra. Gondwana Research 15, 228–242.

Davis, D.W., Williams, I.S., Krough, T.E., 2003. Historical development of U–Pb geochronology. In: Hanchar, J.M., Hoskin, P.W.O. (Eds.), Zircon: Reviews in Mineralogy and Geochemistry, 53, pp. 145–181.

Dickinson, W.R., Gehrels, G.E., 2010. Insights into North American paleogeography and paleotectonics from U–Pb ages of detrital zircons in Mesozoic strata of the Colorado Plateau. International Journal of Earth Sciences 99, 1247–1265.

Embry, A.F., 1991. Mesozoic history of the Arctic Islands. In: Trettin, H.P. (Ed.), The Geology of Canada 3: Geology of the Innuitian Orogen and Arctic Platform of Canada and Greenland. Geological Survey of Canada. Ottawa, Ontario, pp. 371–434.

Embry, A.F., 1992. Crockerland — the northwest source for the Sverdrup Basin, Canadian Arctic Islands. In: Vorren, T.O. (Ed.), Arctic Geology and Petroleum Potential. Norwegian Petroleum Society Special Publication 2. Elsevier, New York, pp. 205–216.

Embry, A., 2011. Petroleum prospectivity of the Triassic–Jurassic succession of Sverdrup Basin, Canadian Arctic Archipelago. In: Spencer, A.M., Embry, A.F., Gautier, D.L., Stoupakova, A.V., Sørensen, K. (Eds.), Arctic Petroleum Geology: Geological Society London Memoir, 35, pp. 545–558. http://dx.doi.org/10.1144/M35.36. 0435-4052/11.

Gaiduk, V.V., 1988. The Middle Paleozoic Vilyui Rift System. Yakutsk, YaF SO AN SSSR, p. 128 (in Russian).

Gehrels, G., 2012. Detrital zircon U–Pb geochronology: current methods and new opportunities. In: Busby, C., Azor, A. (Eds.), Recent Advances in Tectonics of Sedimentary Basins. Wiley-Blackwell, pp. 47–62.

Gelman, M.L., 1963. Triassic diabase association in the Anyui fold zone (Chukotka). Russian Geology and Geophysics 2, 127–134 (in Russian).

Golonka, J., 2011. Phanerozoic palaeoenvironment and palaeolithofacies maps of the Arctic. In: Spencer, A.M., Embry, A.F., Gautier, D.L., Stoupakova, A.V., Sørensen, K. (Eds.), Arctic Petroleum Geology: Geological Society, London, Memoirs, 35, pp. 79–129. http://dx.doi.org/10.1144/M35.6 (0435-4052/11).

Grantz, A., Hart, P.E., Childers, V.A., 2011. Geology and tectonic development of the Amerasia and Canada Basins, Arctic Ocean. In: Spencer, A.M., Embry, A.F., Gautier, D.L., Stoupakova, A.V., Sørensen, K. (Eds.), Arctic Petroleum Geology: Geological Society London Memoir, 35, pp. 771–799. http://dx.doi.org/10.1144/M35.50 (0435-4052/11).

Guynn, J., Gehrels, G., 2010. Comparison of detrital zircon age distributions using the K–S test. https://sites.google.com/a/laserchron.org/laserchron/home/.

Harrison, J.C., St-Onge, M.R., Petrov, O., Strelnikov, S., Lopatin, B., Wilson, P.D., Lynds, T., Shokalsky, S., Hults, C., Bergman, S., Jepsten, H.F., Solli, A., 2008. Geological Map of the Arctic. Geological Survey of Canada, Calgary . Open File 5816.

Henriksen, E., Ryseth, A.E., Larssen, G.B., Heide, T., Ronning, K., Sollid, K., Stoupakova, A.V., 2011. Tectonostratigraphy of the greater Barents Sea: implications for petroleum systems. In: Spencer, A.M., Embry, A.F., Gautier, D.L., Stoupakova, A.V., Sørensen, K. (Eds.), Arctic Petroleum Geology: Geological Society London, Memoir, 35, pp. 163–195. http://dx.doi.org/10.1144/M35.10. 0435-4052/11/$15.00 # The Geological Society of London 2011.

Hoy, T., Lundschien, B.A., 2011. Triassic deltaic sequences in the northern Barents Sea. In: Spencer, A.M., Embry, A.F., Gautier, D.L., Stoupakova, A.V., Sørensen, K. (Eds.), Arctic Petroleum Geology: Geological Society London Memoirs, 35, pp. 249–260. http://dx.doi.org/10.1144/M35.15. 0435-4052/11.

Kostler, J., Sylvester, P.J., 2003. Present trends and the future of zircon in U–Pb geochronology: laser ablation ICPMS. In: Hanchar, J.M., Hoskin, P.W.O. (Eds.), Zircon: Reviews in Mineralogy and Geochemistry, 53, pp. 243–275.

Kuzenkov, N.A., Soboleva, A.A., Matukov, D.I., 2004. The age of the intrusive rocks of Tynagota area (the Subpolar Urals) by data of isotopic age of single zircons. Geology and mineral resources of the European Northeast of Russia, Issue of the XIV Geological congress of Komi Republic, Syktyvkar, II, pp. 98–102 (in Russian).

Kuzmichev, A.B., 2009. Where does the South Anyui suture go in the New Siberian Islands and Laptev Sea? Implications for the Amerasia basin origin. Tectonophysics 463, 86–108.

Kuzmichev, A.B., Goldyrev, A.E., 2007. Permian–Triassic trap magmatism in Bel'kov Island (New Siberian Islands). Russian Geology and Geophysics 48, 167–176.

Kuzmichev, A.B., Pease, L.L., 2007. Siberian trap magmatism on the New Siberian Islands: constraints for Arctic Mesozoic plate tectonic reconstructions. Journal of the Geological Society of London 164, 1–10.

Kuzmichev, A.B., Soloviev, A.V., Gonikberg, V.E., Shapiro, M.N., Zamzhitskii, O.V., 2006. Mesozoic syn-collision siliciclastic sediments, Bol'shoi Lyakhov Island (New Siberian Islands). Stratigraphy and Geological Correlation 14, 30–48.

Lawver, L.A., Grantz, A., Gahagan, L.M., 2002. Plate kinematic evolution of the present Arctic region since the Ordovician. In: Miller, E.L., Grantz, A., Klemperer, S.L. (Eds.), Tectonic evolution of the Bering Shelf–Chukchi Sea–Arctic margin and adjacent landmasses: Geological Society of America Special Paper, 360, pp. 333–358.

Lawver, L.A., Gahagan, L.M., Norton, I., 2011. Paleogeographic and tectonic evolution of the Arctic region during the Paleozoic. In: Spencer, A.M., Embry, A.F., Gautier, D.L., Stoupakova, A.V., Sørensen, K. (Eds.), Arctic Petroleum Geology: Geological Society London Memoir, 35, pp. 61–77. http://dx.doi.org/10.1144/M35.5. 0435-4052/11.

Ledneva, G., Pease, V., Sokolov, S., 2011. Triassic hypabyssal mafic intrusions and associated tholeiitic basalts of the Kolyuchinskaya Bay, Chukotka (NE Russia): links to the Siberian LIP. Journal of Asian Earth Sciences 40, 737–745.

Lorenz, H., Gee, D.G., Whitehouse, M.J., 2007. New geochronologic data on Paleozoic igneous activity and deformation in the Severnaya Zemlya Archipelago, Russia, and implications for the development of the Eurasian Arctic margin. Geological Magazine 144, 105–205.

Lorenz, H., Gee, D.G., Simonetti, A., 2008. Detrital zircon ages and provenance of the Late Neoproterozoic and Palaeozoic successions on Severnaya Zemlya, Kara Shelf: a tie to Baltica. Norwegian Journal of Geology 88, 235–258.

Mariani, R.K., 1987. Petrography and diagenesis of the Ledge Sandstone member of the Triassic Ivishak Formation. In: Bird, K.J., Magoon, L.B. (Eds.), Petroleum Geology of the Northern Part of the Arctic National Wildlife Refuge, Northeastern Alaska: United States Geological Survey Bulletin, 1778, pp. 101–115.

Miller, E.L., Toro, J., Gehrels, G., Amato, J.M., Prokopiev, A., Tuchkova, M.I., Akinin, V.V., Dumitru, T.A., Moore, T.M., Cecile, M.P., 2006. New insights into Arctic paleogeography and tectonics from U–Pb detrital zircon geochronology. Tectonics 25, TC3013–TC3032. http://dx.doi.org/10.1029/2005TC001830.

Miller, E.L., Soloviev, A., Kuzmichev, A., Gehrels, G., Toro, J., Tuchkova, M., 2008. Jurassic and Cretaceous foreland basin deposits of the Russian Arctic: separated by birth of Makarov Basin? Norwegian Journal of Geology 88, 201–226.

Miller, E.L., Gehrels, G.E., Pease, V., Sokolov, S., 2010. Paleozoic and Mesozoic stratigraphy and U–Pb detrital zircon geochronology of Wrangel Island, Russia: constraints on paleogeography and paleocontinental reconstructions of the Arctic. American Association of Petroleum Geologists 94, 665–692. http://dx.doi.org/10,1306/102009036.

Miller, E.L., Kuznitsov, N., Soboleva, A., Udoratina, O., Grove, M.J., Gehrels, G., 2011. Baltica in the Cordillera? Geology 39, 791–794. http://dx.doi.org/10.1130/G31910.1.

Nebel-Jacobsen, Y., Munker, C., Nebel, O., Mezger, K., 2011. Precambrian sources of Early Paleozoic SE Gondwana sediments as deduced from combined Lu–Hf and U–Pb systematics of detrital zircons, Takaka and Buller terrane, South Island, New Zealand. Gondwana Research 20, 427–442.

Nikishin, A.M., Ziegler, P.A., Stephenson, R.A., Cloetingh, S.A.P.L., Furne, A.V., Fokin, P.A., Ershov, A.V., Bolotov, S.N., Korotaev, M.V., Alekseev, A.S., Gorbachev, V.I., Shipilov, E.V., Lankreijer, A., Bembinona, E.Yu., Shalimov, I.V., 1996. Late Precambrian to Triassic history of the East European Craton: dynamics of sedimentary basin evolution. Tectonophysics 268, 23–63.

Nikishin, A.M., Ziegler, R.A., Abbott, D., Brunet, M.F., Cloetingh, S., 2002. Permo–Triassic intraplate magmatism and rifting in Eurasia: implications for mantle plumes and mantle dynamics. Tectonophysics 351, 3–29. http://dx.doi.org/10.1016/S0040-1951(02)00123-3.

Nikishin, V.A., Malyshev, N.A., Nikishin, A.M., Obmetko, V.V., 2011. The Late Permian–Triassic system of rifts of the South Kara Sedimentary Basin, 66. Moscow University Bulletin, pp. 377–384.

Oleshko, B.M., 1981. The 1:200,000 state geologic map of the USSR. The Verkhoyansk Series. Sheets Q-53-XIX-XX. Map and Explanatory notes: Moscow, Soyuzgeolfond, 1-85. (in Russian).

Omma, J.E., Pease, V., Scott, R.A., 2011. U–Pb SIMS zircon geochronology of Triassic and Jurassic sandstones on northwestern Heiberg Island, northern Sverdrup Basin, Arctic Canada. In: Spencer, A.M., Embry, A.F., Gautier, D.L., Stoupakova, A.V., Sørensen, K. (Eds.), Arctic Petroleum Geology: Geological Society London Memoir, 35, pp. 559–566. http://dx.doi.org/10.1144/M35.37. 0435-4052/11.

Pankhurst, M.J., Shaefer, B.F., Betts, P.G., 2010. Geodynamics of rapid voluminous felsic magmatism through time. Lithos 123, 92–101.

Parfenov, L.M., Prokopiev, A.V., Gaiduk, V.V., 1995. Cretaceous frontal thrusts of the Verkhoyansk fold belt, eastern Siberia. Tectonics 14, 342–358. http://dx.doi.org/10.1029/94TC03088.

Pease, V., 2011. Eurasian orogens and Arctic tectonics: an overview. In: Spencer, A.M., Embry, A.F., Gautier, D.L., Stoupakova, A.V., Sørensen, K. (Eds.), Arctic Petroleum Geology: Geological Society London Memoir, 35, pp. 311–324. http://dx.doi.org/10.1144/M35.20. 0435-4052/11.

Pease, V., Scott, R.A., 2009. Crustal affinities in the Arctic Uralides, northern Russia: significance of 11 detrital zircon ages from Neoproterozoic and Palaeozoic sediments in Novaya Zemlya and Taimyr. Journal of the Geological Society of London 166, 1–10. http://dx.doi.org/10.1144/0016-76492008-093.

Pease, V., Kosteva, N., Tebenkov, A., Makarjeva, E., Makarjev, A., 2007. U–Pb zircon provenance of Late Triassic sandstone from Franz Josef Land. In: Brekke, H., Henriksen, S., Haukdal, G. (Eds.), Abstracts and Proceedings of the Geological Society of Norway, ICAM V, NGF IO-096, 123.

Pease, V., Kosteva, N., Tebenkov, A., Makarjeva, E., Makarjev, A., 2012. U–Pb zircon provenance of strata from Franz Josef Island. In: Stone, D.B., Clough, J.G., Thurston, D.K. (Eds.), Abstract Volume, ICAM VI: Geophysical Institute Report UAG-R-335, 161.

Press, W.H., Teukolsky, S.A., Vetterling, W.T., Flannery, B.P., 1992. Numerical Recipes in Fortran: the Art of Scientific Computing. England, Cambridge University Press, Cambridge . 963 p.

Prokopiev, A.V., Tronin, A.V., 2004. Structural and sedimentary features of the zone of junction of the Kular-Nera slate belt and the In'yali-Debin synclinorium. Otechestvennaya Geologiya 4, 49–56 (in Russian).

Prokopiev, A.V., Toro, J., Miller, E.L., Gehrels, G.E., 2008. The paleo-Lena River — 200 m.y. of transcontinental zircon transport in Siberia. Geology 36, 699–702.

Prokopiev, A.V., Toro, J., Hourigan, J.K., Bakharev, A.G., Miller, E.L., 2009. Middle Paleozoic–Mesozoic boundary of the North Asian craton and the Okhotsk terrane: new geochemical and geochronological data and their geodynamic interpretation: European Geoscience Union Stephan Mueller Special Publication, Series, 4, pp. 71–84.

Reichow, M.K., Pringle, M.S., Al'mukhamedov, A.I., Allen, M.B., Andreichev, V.L., Buslov, M.M., Davies, C.E., Fedoseev, G.S., Fitton, J.G., Inger, S., Medvedev, A.Ya., Mitchell, C., Puchkov, V.N., Safonova, I.Yu., Scott, R.A., Saunders, A.D., 2009. The timing and extent of the eruption of the Siberian Traps large igneous province: implications for the end-Permian environmental crisis. Earth and Planetary Science Letters 277, 9–20.

Rino, S., Kon, Y., Sato, W., Maruyama, S., Santosh, M., Zhao, D., 2008. The Grenvillian and Pan-African orogenies: world's largest orogenies through geologic time and their implications on the origin of the superplume. Gondwana Research 14, 51–72.

Safonova, I., Maruyama, S., Hirata, T., Kon, Y., Rino, S., 2010. LA ICP MS U–Pb ages of detrital zircons from Russia largest rivers: implications for major granitoid events in Eurasia and global episodes of supercontinent formation. Journal of Geodynamics 50, 134–153.

Scarrow, J.H., Hetzel, R., Goroshanin, V.M., Dinn, M., Glodny, J., Gerdes, A., Ayala, C., Montero, P., 2002. Four decades of geochronologic work in the southern and middle Urals: A review. In: Brown, D., Juhlin, C., Puchkov, V. (Eds.), Mountain Building in the Uralides: Pangea to the Present: American Geophysical Union Geophysical Monograph, 132, pp. 233–255.

Scott, R., Howard, J., Guo, L., Schekoldin, R., Pease, V., 2010. Offset and curvature of the Novaya Zemlya fold-and-thrust belt, Arctic Russia. In: Vining, B.A., Pickering, S. (Eds.), From mature basins to new frontiers: Geological Society of London Proceedings of the 7th Petroleum Geology Conference, Petroleum Geology Conferences, pp. 645–657.

Sherwood, K.W., Johnston, P.P., Craig, J.D., Zerwick, S.A., Lothamer, R.T., Thurston, D.K., Hurlbert, S.B., 2002. Structure and stratigraphy of the Hanna Trough, U.S. Chukchi Shelf, Alaska. In: Miller, E.L., Grantz, A., Klemperer, S.L. (Eds.), Tectonic evolution of the Bering Shelf–Chukchi Sea–Arctic margin and adjacent landmasses: Geological Society of America Special Paper, 360, pp. 39–66.

Soboleva, A.A., Kulikova, K.V., Morgunova, A.A., Bezinova, L.V., 2008a. Fragments of the pre-Uralian history of the Enganepe Uplift. Bulletin of the Institute of Geology Komi SC UB RAS 7–12 (in Russian).

Soboleva, A.A., Ivanov, V.N., Kuzenkov, N.A., Vasilev, A.K., 2008b. Origin and age of rhyolites from Tynagotsko-Tykotlovsky area (Subpolar Urals). Petrology and mineralogy of the Northern Urals and Timan, Syktyvkar: Proceedings of Institute of Geology KSC UB RAS, 124, pp. 27–51 (in Russian).

Sosunov. G.M., Pavlova O.K., Gel'man M.L., 1982. Geologic map of the Northeast USSR, scale 1:1500000 with legend and explanation. Magadan, 39. (in Russian).

Torsvik, T.H., Andersen, T.B., 2002. The Taimyr fold belt, Arctic Siberia: timing of prefold remagnetisation and regional tectonics. Tectonophysics 352, 335–348.

Tuchkova, M.I., Morozov, O.L., Katkov, S.M., 2007. Lower–Middle Triassic rocks in the Enmynveem River (western Chukotka). Lithology and Mineral Resources 42, 486–502.

Vernikovsky, V.A., Neimark, L.A., Ponomarchuk, V.A., Vernikovskaya, A.E., 1995. Geochemistry and age of collision granitoids and metamorphites of the Kara microcontinent (northern Taimyr). Russian Geology and Geophysics 36, 46–60.

Vernikovsky, V.A., Sal'nikova, E.B., Kotov, A.B., Ponomarchuk, A.B., Kovach, V.P., Travin, A.V., Yakovleva, S.Z., Berezhnaya, N.G., 1998. The age of post-collision granitoids of the North Taimyr: U–Pb, Sm–Nd, Rb–Sr, and Ar–Ar data. Doklady Earth Sciences 363A, 1191.

Vernikovsky, V.A., Pease, V.L., Vernikovskaya, A.E., Romanov, A.P., Gee, D.G., Travin, A.A., 2003. First report of early Triassic A-type granite and syenite intrusions from Taimyr: product of the northern Eurasian superplume? Lithos 66, 23–36.

Vol'nov, D. A., Lopatin, B. G., D. S. Sorokov, D.S., 1999. State geological map of the Russian Federation Scale1:000000 (New Series). Sheet S-53-55 New Siberian Islands. Explanatory Notes, VSEGEI, St. Petersburg (in Russian).

Walderhaug, H.J., Eide, E.A., Scott, R.A., Inger, S., Golionko, E.G., 2005. Paleomagnetism and 40Ar/39Ar geochronology from the South Taimyr igneous complex, Arctic Russia: a Middle–Late Triassic magmatic pulse after Siberian flood-basalt volcanism. Geophysical Journal International 163, 501–517.

Zhulanova, I.L., Rusakova, T.B., Kotlyar, I.N., 2007. Geochronology and geochronometry of Mesozoic endogenic events of northeast Asia. Moscow, Nauka. 358 p. (in Russian).

Ziegler, P.A., 1988. Evolution of the Arctic-North Atlantic and the western Tethys. American Association of Petroleum Geologists Memoir 43. 198 pp.